

This is to certify that the dissertation entitled

Solid State Nuclear Magnetic Resonance Studies of the Influenza Fusion Peptide Associated with Membrane Bilayers

presented by

Paul Parkanzky

has been accepted towards fulfillment of the requirements for the

Ph.D.	degree in _	Chemistry
,	0	1
	Tried P. l.	Jeli kç essor's \$ignature
	Major Profe	essor's \$ignature
	3/24	106
		Date

MSU is an Affirmative Action/Equal Opportunity Institution

LIBRARY Michigan State University

PLACE IN RETURN BOX to remove this checkout from your record. TO AVOID FINES return on or before date due. MAY BE RECALLED with earlier due date if requested.

DATE DUE	DATE DUE	DATE DUE
		,, -
-		
		12,000,000,000,000,000,000

2/05 p:/CIRC/DateDue.indd-p.1

Solid State Nuclear Magnetic Resonance Studies of the Influenza Fusion Peptide Associated with Membrane Bilayers

by

Paul Parkanzky

A DISSERTATION

Submitted to
Michigan State University
in partial fulfillment of the requirements
for the degree of

DOCTOR OF PHILOSOPHY

Department of Chemistry

Abstract

Solid State Nuclear Magnetic Resonance Studies of the Influenza

Fusion Peptide Associated with Membrane Bilayers

by

Paul Parkanzky

Membrane fusion in influenza virus is caused by the influenza viral hemagglutinin protein (HA). The amino terminus of the HA₂ domain of the hemagglutinin protein is known as the 'fusion peptide.' In this work, solid-state nuclear magnetic resonance (NMR) spectroscopy was used to understand the structures of synthetic peptides based on the influenza fusion peptide. Because the free fusion peptide has been shown to induce fusion of liposomes in a pH-dependent way similar to the complete protein, the information gained by the study of the free peptide should be valuable for understanding the mechanism of influenza viral fusion by the influenza fusion protein.

The fusion peptide was synthesized with a solubilizing 'host-sequence'.

The physical properties and biological activities of these peptides were studied to provide evidence that the peptide structures examined were relevant to the larger fusion protein system.

Because the influenza fusion peptide has been studied with a variety of lipid compositions using a number of sample preparation methods, the effects of lipid composition, peptide:lipid ratio, temperature, and pH on the membrane-

bound fusion peptide structure were studied. REDOR subtraction was used to filter out the large natural abundance ¹³C carbonyl signals from the NMR spectra, and chemical shift was used as a convenient indicator of local secondary structure.

The data revealed at least two distinct structures of the membrane bound fusion peptide. The structure is dependent on the lipid and cholesterol composition of the membrane to which the peptide is associated. It was also shown that the fusion peptide causes pH-dependent lipid mixing regardless of its equilibrium structure. This shows that there are at least two distinct structures of the influenza fusion peptide that can induce fusion.

A proposed 3¹⁰ helix proposed to be present in the low pH peptide in DPC detergent solution and in POPC:POPG membranes but absent at neutral pH was probed by REDOR spectroscopy. Our REDOR measurements show that this structural feature is present in fusion peptide bound to DPC micelles and to POPC:POPG membranes at both low and neutral pH. Chemical shift measurements support this conclusion.

In honor of

Lt. Vincent Halloran

Ladder 8

FDNY

Acknowledgements

I would like to thank the members of my group for all of their support and for the many valuable conversations we had over the years. I appreciate all the great help from the staff at MSU, especially Janet and Lisa. I owe a great debt to Dr. Weliky, for sharing his enthusiasm, and for his guidance throughout my project. I really appreciate the time he took to make sure that I learned and understood as much as I could. And finally, I would like to thank my loving wife Kristina. Without her support I don't know where I'd be.

Table of Contents

LIST OF TABLES	viii
LIST OF FIGURES	ix
LIST OF ABBREVIATIONS	xiv
Solid State Nuclear Magnetic Resonance Spectroscopy of Members Associated Fusion Peptide	rane 1
1.1 Introduction	
2. Biological and Physical Properties of the Fusion Peptide	14
2.1 Introduction.2.2 Experimental.2.3 Results and Discussion.2.4 Conclusions.2.5 References.	16 21
3. Conformational Studies of Membrane and Detergent Bound Fusion by Solid State Nuclear Magnetic Resonance Rotational Echo Double Subtraction Methods	Resonance
3.1 Introduction.3.2 Experimental.3.3 Results and Discussion.3.4 Conclusions.3.5 References.	37 40 47
4. Solid State Nuclear Magnetic Resonance Rotational Echo Double Measurements to Probe for a pH Dependent Structural Feature in the Peptide	e Fusion
4.1 Introduction	58 60

5.	Summary and Future Work	73
	5.1 Summary	74
	5.2 References	

List of Tables

Table 1. The amino acid sequences of the N-terminal 20 residues of various strains of influenza hemagglutinin HA_2 . The bottom line illustrates a consensu sequence in which B denotes a hydrophobic residue, G refers to a glycyl (and two cases asparagine) residue, and X denotes a hydrophilic, usually acidic, residue. Boxes enclose the invariant residues	l in
Table 2. Averaged ¹³ C carbonyl chemical shift values (in ppm) of experimental measured chemical shifts categorized according to secondary structural assignment and amino-acid type. (The standard deviation is given in parentheses)	•
Table 3. Summary of REDOR results. Considerable dephasing in DPC micel and POPC:POPG (4:1) lipid membranes at both pH 7.4 and pH 5.0 suggests presence of a 3 ₁₀ helix in the fusion peptide in both environments at both pH's The numbers in parentheses are the uncertainties in the experimental	the

List of Figures

Figure 1. Lipid bilayer showing the phospholipids headgroups and hydrophobic acyl chains which make up the lipids2
Figure 2. The first half of the influenza viral life cycle. The virus enters the cell by endocytosis. The pH drops in the endosome, initiating conformational changes of the hemagglutinin protein on the viral membrane surface. These conformational changes ultimately lead to fusion of the viral and endosomal membranes and release of the viral contents into the cell
Figure 3. Model for fusion by influenza hemagglutinin. At neutral pH the HA ₁ globular head groups sit atop the coiled stalks of HA ₂ . At low pH, the HA ₁ head groups dissociate and HA ₂ adopts an extended coiled coil conformation. This exposes the fusion peptide region of HA ₂ allowing it to interact with the endosomal membrane
Figure 4. Influenza viral fusion has been hypothesized to occur in five steps: (1) pH induced conformational changes and binding with the target membrane; (2) clustering of HA trimers at the fusion site; (3) hemifusion; (4) opening of the fusion pore; (5) dilation of the fusion pore
Figure 5. M_t vs. time for IFP2 with POPC:POPG (4:1), POPC:POPG:Chol (8:2:5), and the LM lipid mixture at pH = 5.0 and 1:150 peptide:lipid mol ratio. After fluorescence intensity has stabilized ~43% lipid mixing was measured for the POPC:POPG and POPC:POPG:Chol lipid mixtures, while ~25% lipid mixing was measured for the LM lipid mixture case
Figure 6. A plot of M_t vs. time for IFP2 with POPC:POPG (4:1) and LM at a 1:75 peptide:lipid ratio. Upon addition of IFP2 to the lipid vesicles at pH = 7.4 lipid mixing was measured. After fluorescence intensity had stabilized, citric acid was added to bring the pH to 5.0. At this point additional lipid mixing occurred23

Figure 8. ¹³C solid state NMR spectra of a sample containing membrane-associated IFP2 peptide at –50 °C. The sample was prepared in 10 mM acetate buffer at pH 5.0 and with peptide:lipid mol ratio of ~ 0.014. The sample was made with POPC:POPG:Chol (8:2:5). The spectra in (a) and (b) are the respective REDOR S₀ and S₁ spectra. Spectrum (c) is the spectrum which results from subtracting the S₁ data from the S₀ data. The displayed REDOR-filtered difference spectrum is dominated by the Leu-2 carbonyl signal. Data were acquired with cross-polarization and with 8 kHz MAS frequency and were processed with 100 Hz Gaussian line broadening and a fifth order polynomial baseline correction. There were 41,344 S₀ and 41,344 S₁ transients.......36

Figure 9. ¹³C solid state NMR spectra of membrane- or detergent-associated fusion peptide samples containing either (a-d) IFP1 peptide or (e-g) IFP2 peptide. Because of Leu-2 ¹³C carbonyl/Phe-3 ¹⁵N labeling of the peptides and the application of a 1.0 ms REDOR filter, the displayed REDOR difference spectra are dominated by Leu-2 carbonyl signals. For the displayed spectra, the peptide was associated with either (a) DPC detergent or the following lipid mixtures: (b, e) POPC:POPG (4:1); (c, f) POPC:POPG:Chol (8:2:5); or (d, g) LM (mixture which reflects the approximate lipid headgroup and cholesterol composition of the target epithelial cells of the virus). The (a, b, e) spectra are dominated by a peak at 177.5 ppm which indicates helical structure near Leu-2. The (d, g) spectra are dominated by a peak at 174.5 ppm which indicates non-helical structure near Leu-2. The (c, f) spectra display significant intensity at both 177.4 and 174.5 ppm which indicates a peptide population with helical structure and a peptide population with non-helical structure near Leu-2. Each sample was prepared in 10 mM acetate buffer at pH 5.0 with a peptide:lipid or peptide:detergent mol ratio of ~ 0.007. Data were acquired using crosspolarization, 8 kHz MAS frequency, and a temperature of either -80 °C (sample a) or -50 °C (samples b-g). Each spectrum was processed with 50 Hz Gaussian line broadening and fifth order polynomial baseline correction. The total $(S_0 + S_1)$ numbers of transients were: (a) 49512; (b) 253952; (c) 121344; (d) 211446; (e) 240192; (f) 286720; (g) 184320......43

Figure 10. Figure 10. Room-temperature ¹³C solid state NMR spectra of membrane-associated Influenza fusion peptide compared with spectra taken at -50 °C. Spectrum (a) is the room temperature spectrum taken using the same sample as used in Figure 9(e), which contained IFP2 associated with POPC:POPG (4:1). For spectrum (b), the sample IFP1 associated with POPC:POPG:Chol (8:2:5) at a peptide to lipid ratio of ~0.14 was used. Spectra (c) and (d) are the -50 °C counterparts to spectra (a) and (b), respectively. REDOR-filtered difference spectra were taken and the observed Leu-2 carbonyl signals are displayed. Spectrum (a) has a similar chemical shift (177.8 ppm) as was observed at -50 °C, which indicates local helical structure. Spectrum (c) has a broad peak with chemical shift overlapping the chemical shifts observed in spectrum (d), suggesting that a similar mixture of structures is present at both -50 °C and at room temperature. Spectrum (a) was collected using a 5 s recycle delay and 4 ms dephasing period. Spectrum (b) was collected using a 2 s recycle delay and 2 ms dephasing period. Spectrum (a) is the result of 35008 total $(S_0 + S_1)$ transients. Spectrum (b) is the result of 80896 transients. Spectrum (c) is the result of 240192 transients, and spectrum (d) is the result of 82688 transients. Spectra (a), (c), and (d) were processed with 50 Hz Gaussian line broadening and spectrum (b) was processed with 100 Hz line broadening. All the spectra were processed using a fifth order polynomial baseline

Figure 11. 13 C solid state NMR spectra of samples containing membrane-associated IFP2 peptide at -50 $^{\circ}$ C. The samples were prepared in 10 mM HEPES/5 mM MES buffer at pH 7.4 and with peptide:lipid mol ratio of \sim 0.007. The samples in spectra (a) and (b) were made with POPC:POPG (4:1) and with LM, respectively. The displayed REDOR-filtered difference spectra are dominated by Leu-2 carbonyl signals. The peak chemical shift in spectrum (a) is 177.5 ppm which indicates predominant helical structure. The peak chemical shift in spectrum (b) is 174.7 ppm which indicates predominant non-helical structure. Data were acquired with cross-polarization and with 8 kHz MAS frequency and were processed with 50 Hz Gaussian line broadening and fifth order polynomial baseline correction. For each spectrum, the total ($S_0 + S_1$) number of transients was 204800.

Figure 12. Solution NMR structure of the influenza fusion peptide in DPC micelles showing an N-terminal alpha helix followed by a bend and a short 3₁₀ helix at low pH. The 3₁₀ helix is absent at neutral pH in this structure.......57

Figure 14. ¹³C solid state NMR REDOR spectra of detergent-associated fusion peptide samples with a peptide:detergent ratio of .014 at pH 7.4 and pH 5.0. Because of Gly-13 ¹³C carbonyl/Gly-16 ¹⁵N labeling of the peptide the majority of the dephasing is the result of the dipolar coupling between Gly-13 and Gly-16. Spectra (a) and (c) are the S₀ spectra for IFP associated with DPC micelles at pH 7.4 and pH 5.0 respectively. Spectra (b) and (d) are the corresponding S₁ spectra. These spectra were taken with a 16 ms REDOR dephasing period. The considerable dephasing present in both spectra indicates strong dipolar coupling between Gly-13 and Gly-16, which is indicative of a hydrogen bond present in a 3₁₀ helix. The spectra were processed with 250 Hz Gaussian line broadening and fifth order polynomial baseline correction. Spectra (a) and (b) are each the result of 198208 transients and spectra (c) and (d) are each the result of 277496 transients.

Figure 16. ¹³ C solid state NMR spectra of membrane-associated IFP at – 50 °C at pH 7.4. Spectra (a) were taken using an 8 ms REDOR dephasing period. Spectra (b) were taken using a 16 ms dephasing period. As in the pH 5.0 cases, the S ₀ spectra are denoted (i) while the S ₁ spectra are marked (ii). Again, the considerable dephasing suggests close proximity between the isotopic labels at the Gly-13 carbonyl carbon and the Gly-16 amide nitrogen. All of the spectra were processed with 100 Hz Gaussian line broadening and a seventh order polynomial baseline correction. The (a) spectra are the result of 122880 S ₀ and S ₁ transients and the (b) spectra are the result of 256000 S ₀ and S ₁ transients
Figure 17. ¹³ C solid state NMR REDOR difference spectra of membrane-associated IFP taken at –50 °C with 8 ms of dephasing. The spectra in (a) and (b) result from the subtraction of the S ₁ data from the S ₀ data from Figure 15(a) and Figure 16(a) respectively. Both spectra were processed with 100 Hz
Gaussian line broadening and a seventh order polynomial baseline

List of Abbreviations

AIDS Acquired Immune Deficiency Syndrome

ATR-FTIR Attenuated Total Reflectance Fourier Transform InfraRed

CD Circular Dichroism

Chol Cholesterol

CP Cross Polarization

CSA Chemical Shift Anisotropy

CW Continuous Wave

DPC DodecylPhosphoCholine

ESR Electron Spin Resonance

EPR Electron Paramagnetic Resonance

FMOC 9-FluorenylMethOxyCarbonyl

FTIR Fourier Transform InfraRed

FWHM Full Width at Half Maximum

HA Influenza Hemagglutinin Protein

HEPES N-2-HydroxyEthylpiperazine-N'-2-EthaneSulfonic Acid

HIV Human Immunodeficiency Virus

IFP Influenza Fusion Peptide

IR InfraRed

LM Lipid Mixture

LUV Large Unilamellar Vesicles

MAS Magic Angle Spinning

MES MorpholineEthaneSulfonic Acid

NMR Nuclear Magnetic Resonance

N-NBD-PE N-(7-Nitro-2,1,3-Benzoxadiazol-4-yl)-PhosphatidylEthanolamine

N-Rh-PE N-(lissamine Rhodamine B sulfonyl)-PhosphatidylEthanolamine

NOE Nuclear Overhauser Effect

Pl Phosphatidyllnositol

POPC 1-Palmitoyl-2-Oleoyl-sn-glycero-3-PhosphoCholine

POPE 1-Palmitoyl-2-Oleoyl-sn-glycero-3-PhosphoEthanolamine

POPG 1-Palmitoyl-2-Oleoyl-sn-glycero-3-[Phospho-rac-(1-Glycerol)]

POPS 1-Palmitoyl-2-Oleoyl-sn-Glycero-3-[Phospho-L-Serine]

PPM Parts Per Million

REDOR Rotational-Echo Double-Resonance

RET Resonance Energy Transfer

RF Radio Frequency

SDS Sodium Dodecyl Sulfate

TPPM Two-Pulse Phase-Modulation

UV Ultra-Violet

Chapter One

Solid State Nuclear Magnetic Resonance Spectroscopy of Membrane Associated Fusion Peptides

Solid State Nuclear Magnetic Resonance Spectroscopy of Membrane Associated Fusion Peptide

1.1 Introduction

Cells are separated by membrane bilayers that are composed of phospholipids, cholesterol, and various proteins. Phospholipids are molecules

that are composed of a polar head group and a hydrophobic acyl tail (Figure 1). Membrane fusion is the process by which two membranes join together to become one membrane.

Membrane fusion is required for cell fusion and for fusion between cellular components, which are critical processes in the life cycles of higher organisms. Fusion is also essential to the viral life cycle of enveloped viruses that cause

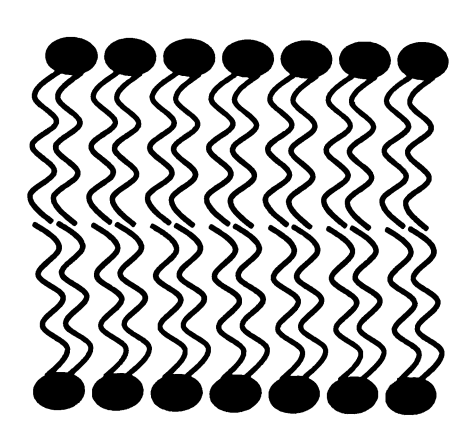


Figure 1. Lipid bilayer showing the phospholipids headgroups and hydrophobic acyl chains which make up the lipids.

diseases such as influenza, chicken pox, Measles (Rubeola), and AIDS (HIV). In influenza, the virus particle is encapsulated by a lipid bilayer, which it acquires upon budding from an infected cell[1]. In pH dependent fusion, such as that which occurs with influenza, the virus first binds to sialic acid containing receptors on the host cell surface and enters the host cell membrane through endocytosis (Figure 2) [2]. Once inside the endosome, fusion of the viral membrane with the endosomal membrane is required to release the virus into the

cytoplasm and to allow insertion of the viral genetic material into the host genome. The low pH (~5.2) inside the endosome initiates structural changes in the hemagglutinin HA protein and leads to fusion of the viral membrane with the endosomal membrane. The final result is release of the viral nucleocapsid into the host cell cytoplasm.

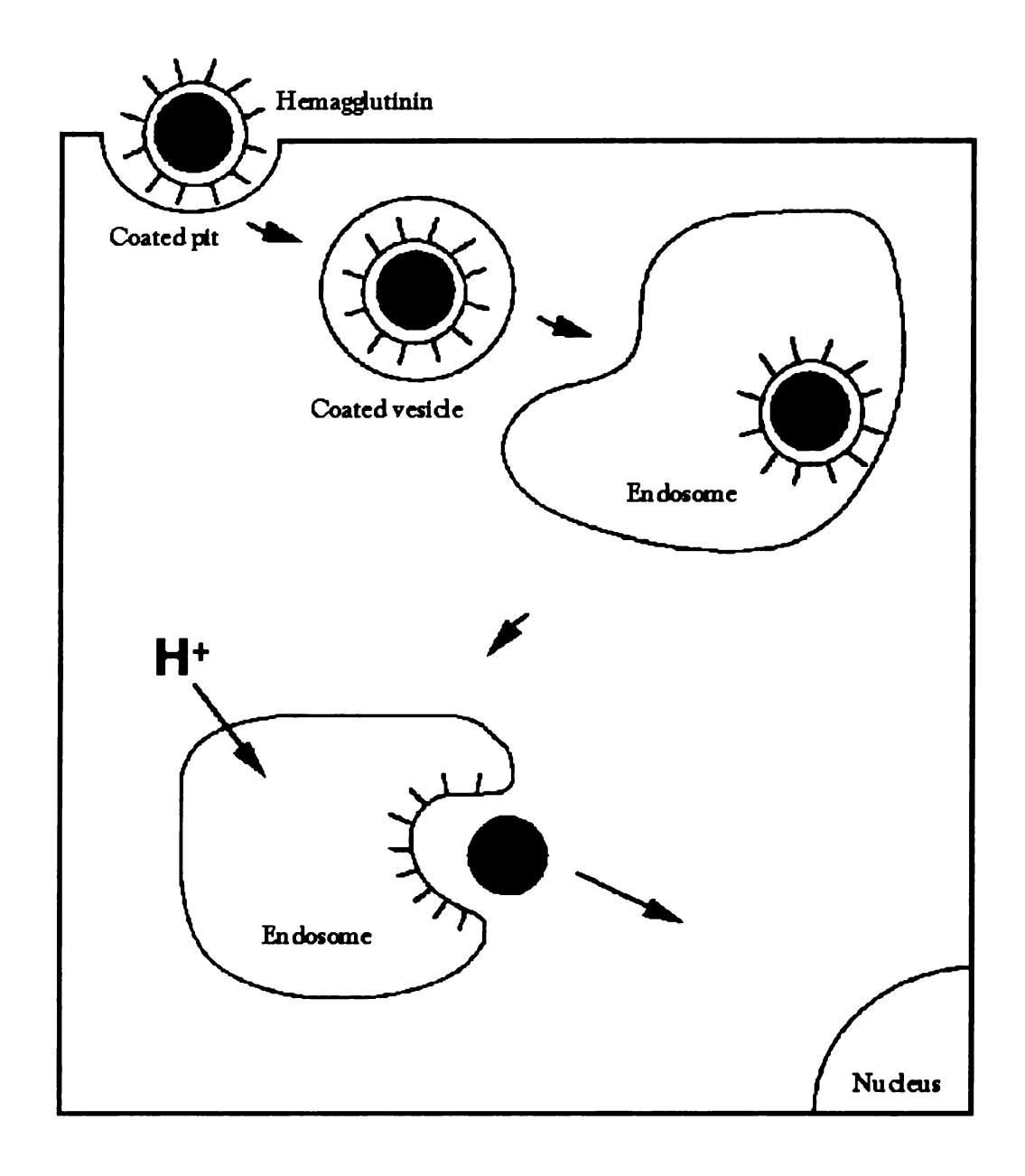


Figure 2. The first half of the influenza viral life cycle. The virus enters the cell by endocytosis. The pH drops in the endosome, initiating conformational changes of the hemagglutinin protein on the viral membrane surface. These conformational changes ultimately lead to fusion of the viral and endosomal membranes and release of the viral contents into the cell.

The most abundant protein in the influenza viral membrane is influenza viral hemagglutinin protein (HA), which plays two important roles in viral replication: (1) it mediates binding of virus particles to cells for endocytosis by binding to receptors that contain sialic acid on the target cell membranes; and (2) it facilitates fusion of the viral and cellular membranes[1].

The amino terminus of the HA₂ domain of the hemagglutinin protein is known as the 'fusion peptide' because mutations or deletions in this region greatly disrupt viral/host cell membrane fusion and infection[3-6]. Radioactive labeling has shown that the fusion peptide is the only region of the influenza viral fusion protein which inserts deeply into membranes during fusion[7]. Peptides with the sequence of the fusion peptide have been shown to have pH-dependent fusion activity similar to that induced by the parent virus, which infers that these peptides are a good model for study of membrane fusion in influenza[2, 8-10].

Understanding the structure of the fusion peptide in the membrane will help to illuminate the viral fusion phenomenon. A better understanding of the mechanism of viral fusion can lead to therapeutic treatments aimed at inhibiting viral fusion. An example of this can be seen in the HIV anti-fusion therapeutic T-20 (enfuvirtide, Fuzeon), which received FDA marketing approval in 2003.

Because viral fusion in influenza is induced by a simple change in pH rather than binding to host cell proteins (as in the case of HIV), influenza has served as the most studied system for fusion research. Studies of pH-dependent influenza fusion and fusion protein structural study allow probing of the relationship between structure and function without the use of mutant analogues.

Influenza viral hemagglutinin protein is synthesized as an inactive homotrimeric glycoprotein precursor, called HA₀, in infected cells[11]. HA₀ becomes fusion active after cleavage into two subunits, HA₁ and HA₂, which are joined by a single disulphide bond (Figure 3)[12].

At neutral pH, the so-called 'fusion peptide' region at the N-terminus of the HA₂ domain is tucked inside of the protein, nearly 100 angstroms from the top of the molecule[13]. Once engulfed by the cell, the low pH of the endosome initiates conformational changes in the influenza hemagglutinin protein (HA) which initiate viral fusion. These conformational changes are such that the fusion peptide region of the HA₂ domain becomes exposed. The HA₂ domain then adopts a coiled-coil conformation and the HA₁-HA₂ disulfide bond is cleaved, and the HA₁ head groups dissociate (Figure 3)[14-16].

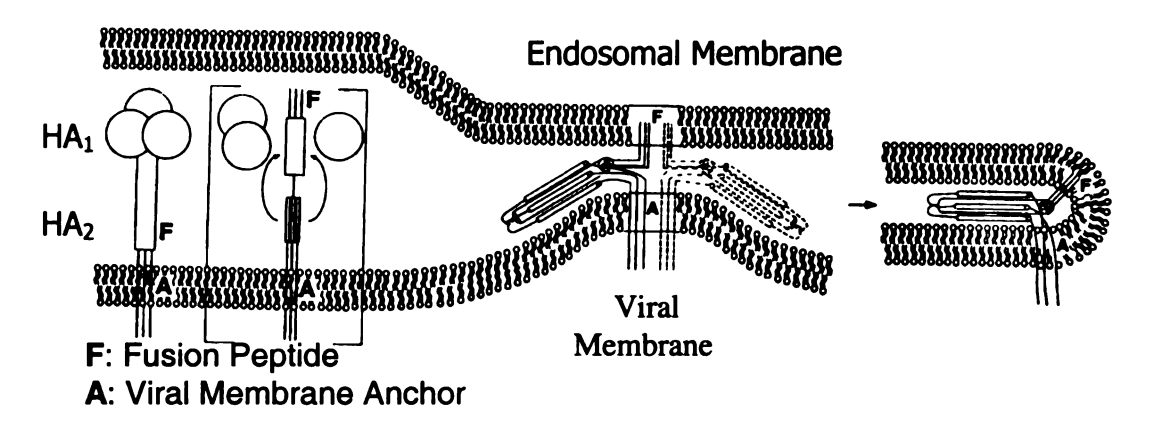


Figure 3. Model for fusion by influenza hemagglutinin. At neutral pH the HA₁ globular head groups sit atop the coiled stalks of HA₂. At low pH, the HA₁ head groups dissociate and HA₂ adopts an extended coiled coil conformation. This exposes the fusion peptide region of HA₂ allowing it to interact with the endosomal membrane.

Influenza viral fusion has then been hypothesized to occur in five steps (Figure 4): (1) pH induced conformational changes and binding with the target membrane; (2) clustering of HA trimers at the fusion site; (3) hemifusion; (4) opening of the fusion pore; (5) dilation of the fusion pore[17].

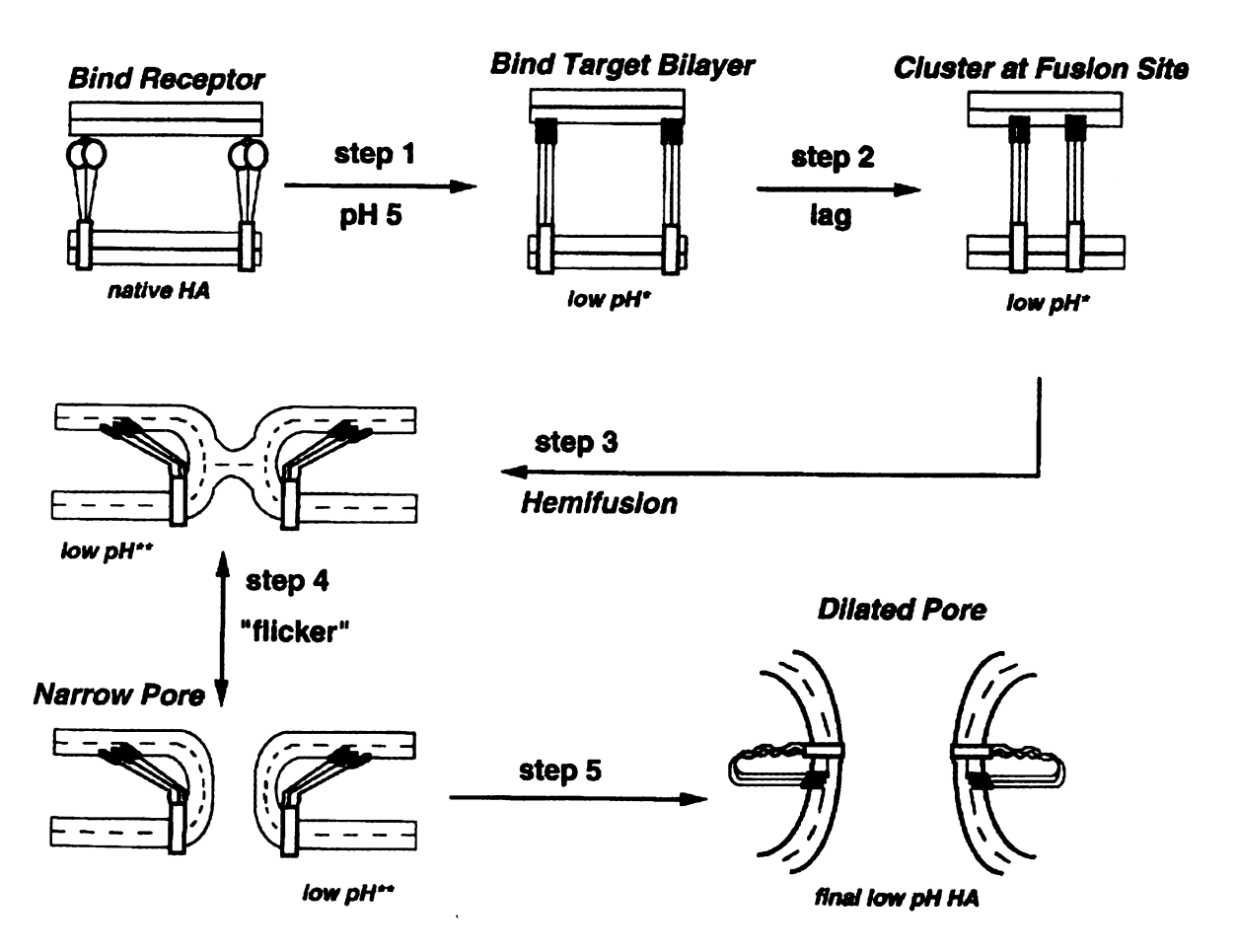


Figure 4. Influenza viral fusion has been hypothesized to occur in five steps: (1) pH induced conformational changes and binding with the target membrane; (2) clustering of HA trimers at the fusion site; (3) hemifusion; (4) opening of the fusion pore; (5) dilation of the fusion pore.

While HA₂ N-terminal fusion peptide sequences from different strains of influenza show somewhat variable sequences (65% overall sequence homology), they exhibit extremely high conservation of 'residue nature,' having

hydrophobic residues, hydrophilic (and usually acidic, but if not acidic, neutral) residues, and small (glycine or asparagines) residues, at invariant positions in the sequence (Table 1)[10].

<u>Strain</u>																					
X31F/68	Gly	Leu	Phe	Gly	Ala	Ile	Ala	Gly	Phe	Ile	Glu	Asn	Gly	Тгр	Glu	Gly	Met	Ile	Asp	Gly	
VIC/75	Gly	Ile	Phe	Gly	Ala	Ile	Ala	Gly	Phe	Ile	Glu	Asn	Gly	Тгр	Glu	Gly	Met	Ile	Asp	Gly	
PR/8/34	Gly	Leu	Phe	Gly	Ala	Ile	Ala	Gly	Phe	Ile	Glu	Gly	Gly	Тгр	Thr	Gly	Met	Ile	Asp	Gly	
Jap/57	Gly	Leu	Phe	Gly	Ala	Ile	Ala	Gly	Phe	Ile	Glu	Gly	Gly	Тгр	Glu	Gly	Met	Val	Asp	Gly	
PPV/34	Gly	Leu	Phe	Gly	Ala	Ile	Ala	Gly	Phe	Ile	Glu	Gly	Gly	Тгр	Glu	Gly	Leu	Val	Asp	Gly	
B/Lee/40	Gly	Phe	Phe	Gly	Ala	Ile	Ala	Gly	Phe	Leu	Glu	Gly	Gly	Тгр	Glu	Gly	Met	Ile	Ala	Gly	
Consensus	G	В	В	G	В	В	В	G	В	В	X	G	G	В	X	G	В	В	X	G	

Table 1: The amino acid sequences of the N-terminal 20 residues of various strains of influenza hemagglutinin HA₂. The bottom line illustrates a consensus sequence in which B denotes a hydrophobic residue, G refers to a glycyl (and in two cases asparagine) residue, and X denotes a hydrophilic, usually acidic, residue. Boxes enclose the invariant residues.

A crystal structure of the low-pH activated HA₂ domain exists for residues 34-176, but atomic resolution structural data for the membrane bound form of the N-terminus fusion peptide of HA₂ is absent[11,18]. The insertion angle of the peptide has also been studied by FTIR and the peptide has been reported to insert at various angles ranging from parallel to oblique relative to the membrane normal, depending upon sample and sample preparation conditions[19]. ATR-FTIR of the fusion peptide, and of fusion-active fusion peptide analogues, in both hydrated and dry egg phosphatidylcholine membranes at neutral and acidic pH, have shown insertion angles between 45 and 70 degrees relative to the membrane normal[20-22]. Circular Dichroism spectroscopy has suggested that the influenza fusion peptide is inserted into micelles predominantly as a helix at

the pH of fusion[23]. A solution NMR structure of the fusion peptide in both sodium dodecyl sulfate (SDS) and dodecylphosphocholine (DPC) micelles has been determined, and shows predominantly helical structure[24, 25]. There is also evidence for helical structure for the fusion peptide in lipid vesicles[26]. EPR studies revealed a helical structure with a maximum insertion depth of 15 angstroms from the lipid phosphate group and a helix tilt angle of ~65° from the membrane normal at both neutral and acidic pH[27].

1.2 References

- 1. Hughson, F.M., *Structural Characterization of Viral Fusion Proteins*. Current Biology, 1995. **5**(3): p. 265-74.
- 2. Murata, M., Y. Sugahara, S. Takahashi, S-i. Ohnishi, pH-Dependent Membrane Fusion Activity of a Synthetic Twenty Amino Acid Peptide with the Same Sequence as That of the Hydrophobic Segment of Influenza Virus Hemagglutinin. Journal of Biochemistry, 1987. 102: p. 957-62.
- 3. Daniels, R.S., J. C. Downie, A. J. Hay, M. Knossow, J. J. Skehel, M. L. Wang, and D. C. Wiley, *Fusion Mutants of the Influenza Virus Hemagglutinin Glycoprotein*. Cell, 1985. **40**: p. 431 439.
- 4. Gething, M.J., R. W. Doms, D. York, and J. White, Studies on the Mechanism of Membrane Fusion: Site-Specific Mutagenesis of the Hemagglutinin of Influenza Virus. Journal of Cell Biology, 1986. 102: p. 11 23.
- 5. Olrich, M., and R. Rott, *Thermolysin Activation Mutants with Changes in the Fusogenic Region of an Influenza Virus Hemagglutinin.* Journal of Virology, 1994. **68**: p. 7537 7539.
- 6. Walker, J.A., and Y. Kawaoka, *Importance of Conserved Amino Acids at the Cleavage Site of teh Haemagglutinin of a Virulant Avian Influenza A Virus*. Journal of General Virology, 1993. **74**: p. 311 314.
- 7. Durrer, P., et al., *H+-induced membrane insertion of influenza virus hemagglutinin involves the HA2 amino-terminal fusion peptide but not the coiled coil region*. J Biol Chem, 1996. **271**(23): p. 13417-21.
- 8. Qiao, H., R. Todd Armstrong, Grigory B. Melikyan, Fredric S. Cohen, and Judith M. White, *A Specific Point Mutant at Position 1 of the Influenza Hemagglutinin Fusion Peptide Displays a Hemifusion Phenotype.*Molecular Biology of the Cell, 1999. **10**: p. 2759 2769.
- 9. Wharton, S.A., S. R. Martin, R. W. Ruigrok, J. J. Skehel, and D. C. Wiley, Membrane Fusion by Peptide Analogues of Influenza Virus Haemagglutinin. Journal of General Virology, 1988. **69**: p. 1847 - 1857.

- 10. Lear, J.D., W. F. DeGrado, *Membrane Binding and Conformational Properties of Peptides Representing the NH₂ Terminus of Influenza HA-2.* The Journal of Biological Chemistry, 1987. **262**(14): p. 6500-05.
- 11. Wilson, I.A., J.J. Skehel, and D.C. Wiley, *Structure of the haemagglutinin membrane glycoprotein of influenza virus at 3 A resolution*. Nature, 1981. **289**(5796): p. 366-73.
- 12. Zhou, Z., J. C. Macosko, D. W. Hughes, B. G. Sayer, J. Hawes, and R. M. Epand, ¹⁵N NMR Study of the Ionization Properties of the Influenza Virus Fusion Peptide in Zwitterionic Phospholipid Dispersions. Biophysical Journal, 2000. **78**: p. 2418-25.
- 13. Kim, C.H., et al., On the dynamics and confirmation of the HA2 domain of the influenza virus hemagglutinin. Biochemistry, 1996. **35**(17): p. 5359-65.
- 14. Bentz, J., *Membrane Fusion Mediated by Coiled Coils: A Hypothesis.* Biophysical Journal, 2000. **78**: p. 886-900.
- 15. Durell, S.R., et al., What studies of fusion peptides tell us about viral envelope glycoprotein-mediated membrane fusion (review). Mol Membr Biol, 1997. **14**(3): p. 97-112.
- 16. W. Weissenhorn, A.D., S. C. Harrison, J. J. Skehel & D. C. Wiley, *Atomic structure of the ectodomain from HIV-1 gp41*. Nature, 1997. **387**(6631): p. 426 431.
- 17. Hernandez, L.D., L. R. Hoffman, T. G. Wolfsberg, and J. M. White, *Virus-Cell and Cell-Cell Fusion*. Annual Reviews of Cell and Developmental Biology, 1996. **12**: p. 627-61.
- 18. Chen, J., J. Skehel, and D. C. Wiley, *N- and C-terminal residues combine in the fusion-pH influenza hemagglutinin HA₂ subunit to form an <i>N cap that terminates the triple-stranded coiled coil.* Proceedings of the National Acadamy of Sciences of the United States of America, 1999. **96**: p. 8967-72.

- 19. Gray, C., S. A. Tatulian, S. A. Wharton, and L. K. Tamm, *Effect of the N-Terinal Glycine on the Secondary Structure, Orientation, and Interaction of the Influenza Hemagglutinin Fusion Peptide with Lipid Bilayers*.

 Biophysical Journal, 1996. **70**: p. 2275-86.
- 20. Ishiguro, R., Noriyuki Kimura, and Sho Takahashi, *Orientation of Fusion-Active Synthetic Peptides in Phospholipid Bilayers: Determination by Fourier Transform Infrared Spectroscopy.* Biochemisty, 1993. **32**: p. 9792 9797.
- 21. Ishiguro, R., Mutsuo Matsumoto, and Sho Takahashi, *Interaction of Fusogenic Synthetic Peptide with Phospholipid Bilayers: Orientation of the Peptide alpha-Helix and Binding Isotherm.* Biochemistry, 1996. **35**: p. 4976 4983.
- 22. Lunenberg, J., Isabelle Martin, Frank Nussler, Jean-Marie, Ruysschaert, and Andreas Herrmann, *Structure and Topology of the Influenza Virus Fusion Peptide in Lipid Bilayers.* The Journal of Biological Chemistry, 1995. **270**(46): p. 27606 27614.
- 23. Chang, D.-K., S-F. Cheng, V. D. Trivedi, and S-H. Yang, *The Aminoterminal Region of the Fusion Peptide of Influenza Virus hemagglutinin HA2 Inserts into Sodium Dodecyl Sulfate Micelle with Residues 16-18 at the Aqueous Boundary at Acidic pH.* The Journal of Biological Chemistry, 2000. **275**(25): p. 19150-58.
- 24. Han, X., Bushweller, J. H., Cafiso, D. S., Tamm, L. K., *Membrane* structure and fusion-triggering conformational change of the fusion domain from influenza hemagglutinin. Nat Struct Biol, 2001. **8**(8): p. 715-20.
- 25. Tamm, L.K., Frits Abildgaard, Ashish Arora, Heike Blad, John H. Bushweller, Structure, Dynamics and Function of the outer Membrane Protein A (OmpA) and influenza Hemagglutinin Fusion Domain in Detergent Micelles by Solution NMR. FEBS Lett, 2003. **555**: p. 139 143.
- 26. Han, X., L. K. Tamm, *A host-guest system to study structure-function relationships of membrane fusion peptides*. Proceedings of the National Acadamy of Science, 2000. **97**(24): p. 13097-102.

27. Macosko, J.C., C.H. Kim, and Y.K. Shin, *The membrane topology of the fusion peptide region of influenza hemagglutinin determined by spin-labeling EPR.* J Mol Biol, 1997. **267**(5): p. 1139-48.

Cl	ha	pl	te	r 2
----	----	----	----	-----

Biological and Physical Properties of the Fusion Peptide

2. Biological and Physical Properties of the Fusion Peptide.

2.1 Introduction

The fusion peptide region of the HA₂ domain of the Influenza hemagglutinin protein has been the focus of considerable study because of its importance in the viral fusion process, as described in chapter one. It is necessary to show that the host-linked fusion peptides used in this work are biologically relevant by demonstrating that they will induce liposome fusion.

This work was done with the consensus Influenza Fusion Peptide (IFP) sequence of H-Gly-Leu-Phe-Gly-Ala-Ile-Ala-Gly-Phe-Ile-Glu-Asn-Gly-Trp-Glu-Gly-Met-Ile-Asp-Gly-Host-NH₂, where the Host sequence consisted of either Gly-Lys-Lys-Lys (IFP1) or Gly-Gly-Lys-Lys-Lys-Trp-Lys-Trp-Lys (IFP2). The glycines in the host sequence served as a flexible linker between the host sequence and the fusion peptide, the lysines increased the peptide's aqueous solubility, and the tryptophans served as UV chromophores for peptide quantitation[1, 2].

To confirm the relevance of these host-linked peptides, resonance energy transfer experiments were performed to test the ability of the synthetic peptides to induce lipid mixing in liposomes. The pH-dependent fusion activity of the host-linked fusion peptides provides evidence that the peptides are a reasonable model for the study of viral fusion in influenza. They will also allow us to correlate structure with at least one measure of fusion peptide function.

Membrane fusion mediated by the influenza virus hemagglutinin has been demonstrated to require at least three hemagglutinin trimers [3]. Because fusion peptide oligomerization is often associated with beta-structure, analytical ultracentrifugation was used to study the peptide aggregation state in aqueous solution. This will allow us to determine whether any large beta-sheet oligomers found in the membrane bound fusion peptide result from the binding of large oligomers from solution, or from the aggregation of the peptide in the lipid membrane.

2.2 Experimental

Materials.

Rink amide resin was purchased from Advanced Chemtech (Louisville, KY), and 9-fluorenylmethoxycarbonyl (FMOC)-amino acids were obtained from Peptides International (Louisville, KY). Isotopically labeled amino acids were purchased from either Cambridge (Andover, MA) or Icon (Summit, NJ) and were FMOC-protected using literature procedures[4, 5]. 1-palmitoyl-2-oleoyl-sn-glycero-3-phosphocholine (POPC), 1-palmitoyl-2-oleoyl-sn-glycero-3-phosphoethanolamine (POPE), 1-palmitoyl-2-oleoyl-sn-glycero-3-[Phospho-L-Serine] (POPS), phosphatidylinositol (PI), sphingomyelin, and 1-palmitoyl-2-oleoyl-sn-glycero-3-[phospho-rac-(1-glycerol)] (POPG) were purchased from Avanti Polar Lipids, Inc. (Alabaster, AL). N-2-hydroxyethylpiperazine-N'-2-

ethanesulfonic acid (HEPES) was obtained from Sigma. All other reagents were analytical grade.

Peptides.

IFP1 fusion peptide (sequence GLFGAIAGFIENGWEGMIDGGKKK) and IFP2 fusion peptide (sequence GLFGAIAGFIENGWEGMIDGGGKKKKWKWK) were synthesized with the 20 N-terminal residues of the Influenza A hemagglutinin fusion protein followed by a 'host sequence' to improve solubility.[1] IFP2 was synthesized with additional lysines and tryptophans to increase the 280 nm absorbance for analytical ultracentrifugation studies and for greater aqueous solubility. Both peptides were synthesized as their C-terminal amides using an automated peptide synthesizer (ABI 431A, Foster City, CA) equipped for FMOC chemistry and were ¹³C carbonyl labeled at Leu-2 and amide ¹⁵N labeled at Phe-3.

Peptide concentrations were quantitated using 280 nm absorbance. The UV assays were calibrated with quantitative amino acid analysis. The extinction coefficient for IFP1 at 280 nm was 7490 M⁻¹cm⁻¹ and the extinction coefficient for IFP2 at 280 nm was 21490 M⁻¹cm⁻¹.

Lipid Preparation.

The "LM" mixture contained POPC, POPE, POPS, sphingomyelin, PI and cholesterol in a 10:5:2:2:1:10 mol ratio. The POPC:POPG lipid mixture contained POPC:POPG in a 4:1 mol ratio. The POPC:POPG:Cholesterol lipid mixture contained POPC:POPG:Cholesterol in a 8:2:5 mol ratio. The LM mixture was chosen to resemble the head group composition of the membranes of cells infected by influenza[6]. The POPC:POPG mixture was chosen because other groups had used this composition. The POPC:POPG:Cholesterol lipid mixture was used so that the affect of Cholesterol on the structure and function of the fusion peptide could be studied. Preparation of large unilamellar vesicles (LUVs) began with dissolution of lipid and cholesterol powders in chloroform. The chloroform was removed under a stream of nitrogen followed by overnight vacuum pumping. Lipid dispersions were formed by addition of buffer followed by homogenization with ten freeze-thaw cycles. LUVs were subsequently prepared by extrusion at least thirty times through a 100 nm filter [7].

Peptide to lipid binding was tested using a 31 ml solution containing ~.33 μmol of peptide. A 1 mL solution was prepared which contained ~50 μmol extruded unilamellar vesicles (LUVs). This vesicle solution was added to the peptide solution and the mixture was kept at room temperature overnight to allow for peptide/lipid binding. Ultracentrifugation of the peptide/lipid mixture at 150,000g for 5 h pelleted the peptide/lipid complex. 280 nm absorbance

measurements of the supernatent showed no remaining peptide, indicating quantitative binding of the peptide to the lipid.

Lipid Mixing Assay for Membrane Fusion.

The resonance energy transfer (RET) assay of Struck et al. was used to monitor inter-vesicle lipid mixing which is one consequence of vesicle fusion[8]. Two types of 100 nm diameter large unilamellar vesicles (LUVs) were prepared. One set contained 2 mol % of the fluorescent lipid N-NBD-PE and 2 mol % of the quenching lipid N-Rh-PE while the other set only contained unlabeled lipids. The fluorescently labeled and unlabeled vesicles were mixed in a 1:9 mol ratio. Following addition of the fusion peptide, lipid mixing between labeled and unlabeled vesicles caused an increase in the average fluorophore-quencher distance with resulting increased fluorescence. Fluorescence was recorded using 4 nm bandwidth on an Instruments S. A. Fluoromax-2 (Edison, NJ) spectrofluorometer operating at excitation and emission wavelengths of 465 and 530 nm, respectively. A quartz cuvette was used with continuous stirring in a water-jacketed cuvette holder. Measurements were carried out at 37 °C with 1.95 ml of 150 µM lipid LUVs in 5 mM HEPES/10 mM MES buffer at pH 5.0 or pH 7.4. 50 µL of peptide solution with initial concentration of 100 µM was added to the vesicle solution to achieve the desired peptide:lipid mol ratio, and the change in fluorescence of the sample was monitored following this addition. The fluorescence was monitored until a constant fluorescence was reached, and then

20 μL of 10% (w/v) Triton X-100 was added, which completely solubilized the liposomes and gave maximum fluorescence.

In the case of the lipid mixing assay experiments in which a pH change was studied, the liposomes were initially made in 5 mM HEPES/10 mM MES buffer at pH 7.4. Peptide was added and fluorescence intensity was monitored until constant fluorescence was reached. The pH was then adjusted to 5.0 with the addition of 11.1 µL of 1 M citric acid. The fluorescence was again monitored until a constant fluorescence was reached, at which point 20 µL of 10% (w/v) Triton X-100 was added, which completely disrupted the liposomes.

The initial residual fluorescence intensity, F_0 , referenced zero lipid mixing. After addition of the peptide, the fluorescence F(t) was monitored as a function of time (t). The maximum fluorescence intensity, F_{max} , was obtained following addition of 20 μ l of 10% Triton X-100. Percent lipid mixing at time t is denoted as M(t) and was calculated using:

$$M(t) = [(F(t) - F_0)/(F_{max} - F_0)] \times 100$$

When the peptide or Triton solution is added to the liposome solution there are two effects on fluorescence: (1) increase due to lipid mixing and (2) decrease due to larger solution volume and resulting lower fluorophore concentration. In calculating M(t), F(t) and F_{max} values were adjusted to take into account the small volume changes that occur upon addition of peptide and detergent. Given

sufficient time, M(t) reached a constant value that is denoted as M_t , the final extent of lipid mixing. M_t was used as a measure of peptide fusogenicity.

At least two runs were made for each measurement and the $M_{\rm f}$ values for the two runs were usually within 2% of each other.

Analytical Ultracentrifugation.

A 20 µM solution of IFP2 in 10 mM pH 5.0 acetate buffer was spun at speeds between 30,000 and 35,000 rpm in a Beckman XLA analytical ultracentrifuge using a An-60 Ti rotor. Samples were loaded into six-channel epon charcoal-filled centerpieces, using quartz windows. Sedimentation equilibrium experiments were performed at 25 °C and peptide distribution was detected with 280 nm absorbance. Data were fitted using software from Beckman/MicroCal.

2.3 Results and Discussion

Lipid Mixing Assays.

Figure 5 displays plots of M_t vs. time for IFP2 added to POPC:POPG (4:1), POPC:POPG:Chol (8:2:5) and the LM lipid mixture at a 1:150 peptide:lipid mol ratio.

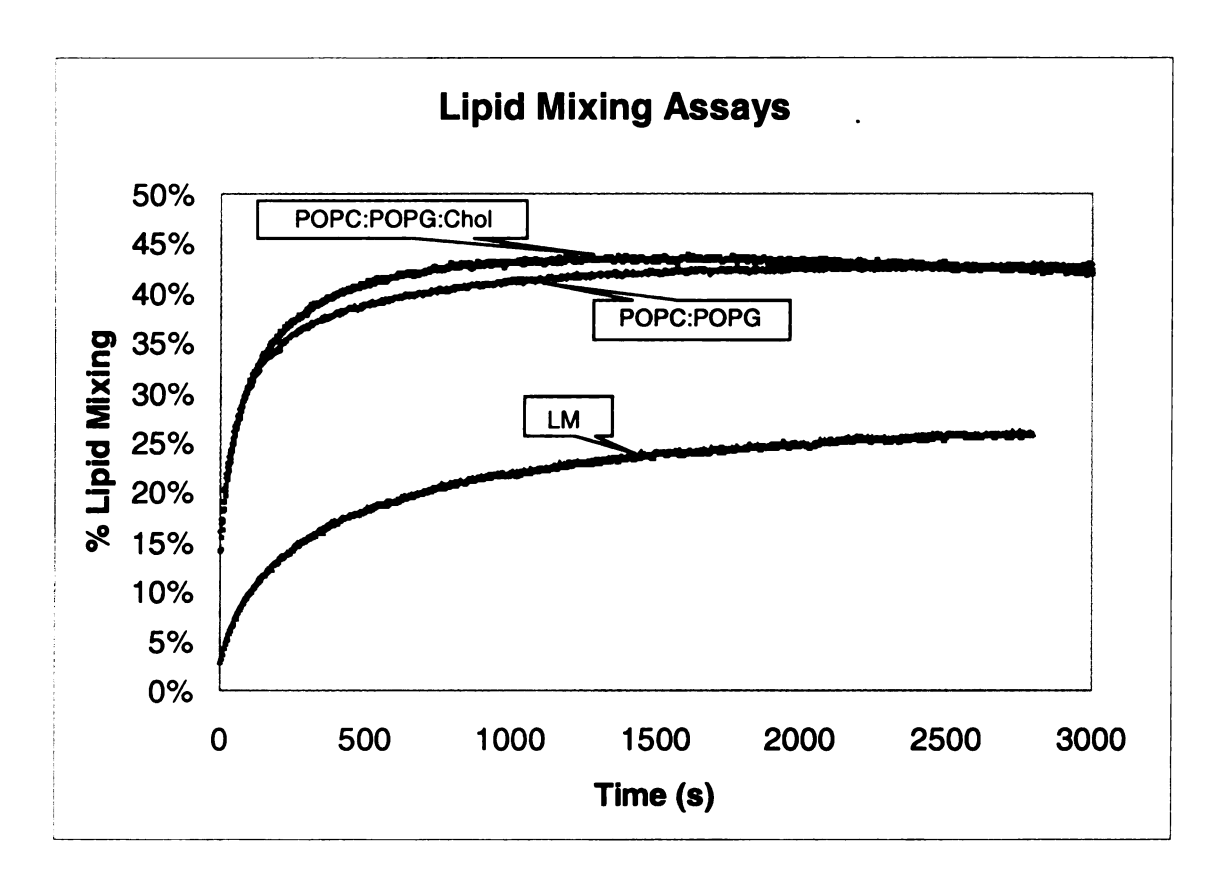


Figure 5. M_t vs. time for IFP2 with POPC:POPG (4:1), POPC:POPG:Chol (8:2:5), and the LM lipid mixture at pH = 5.0 and 1:150 peptide:lipid mol ratio. After fluorescence intensity has stabilized ~43% lipid mixing was measured for the POPC:POPG and POPC:POPG:Chol lipid mixtures, while ~25% lipid mixing was measured for the LM lipid mixture case.

This shows that the influenza fusion peptide is able to induce lipid mixing in liposomes made with the lipid mixtures studied in this work.

Figure 6 displays a plot of M_t vs. time for IFP2 which shows that lipid mixing is induced by IFP2 in POPC:POPG (4:1) and in LM in a pH dependent way.

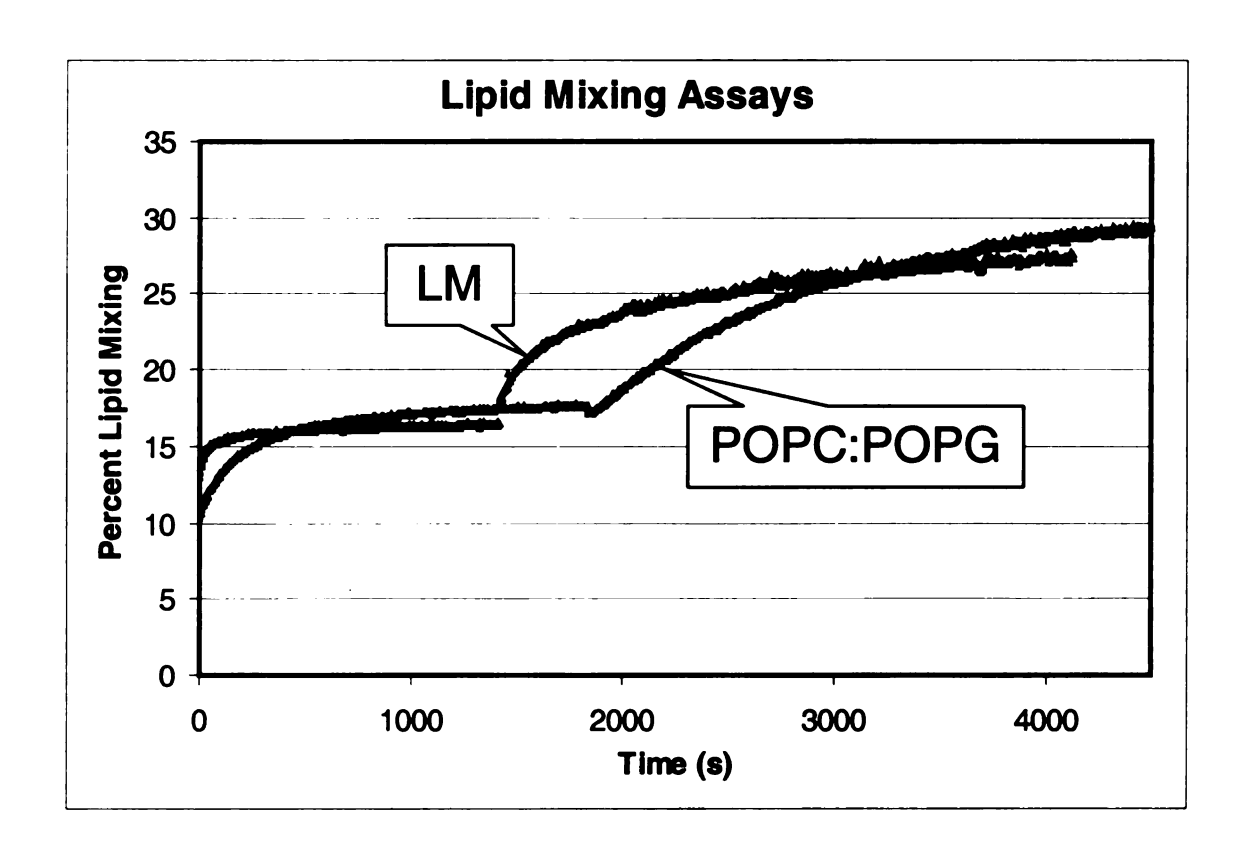


Figure 6. A plot of M_t vs. time for IFP2 with POPC:POPG (4:1) and LM at a 1:75 peptide:lipid ratio. Upon addition of IFP2 to the lipid vesicles at pH = 7.4 lipid mixing was measured. After fluorescence intensity had stabilized, citric acid was added to bring the pH to 5.0. At this point additional lipid mixing occurred.

This pH dependence is similar to the pH dependence of lipid mixing in the case of the full HA₂ fusion protein, but it is difficult to relate the two behaviors, because the fusion peptide is buried inside the fusion protein at neutral pH and exposed at low pH. In another study, it was shown that a larger, 1-127 amino acid fragment of the fusion protein also promoted lipid mixing in a pH dependent way despite the fusion peptide being exposed at both neutral and low pH in that construct[9]. This pH dependent function of the fusion peptide allows us to

correlate peptide structure to functional fusion activity without making mutant peptides.

Analytical Ultracentrifugation.

Figure 7 displays equilibrium analytical ultracentrifugation data and fitting for a 20 μ M solution of IFP2 in 10 mM acetate buffer with pH 5.0.

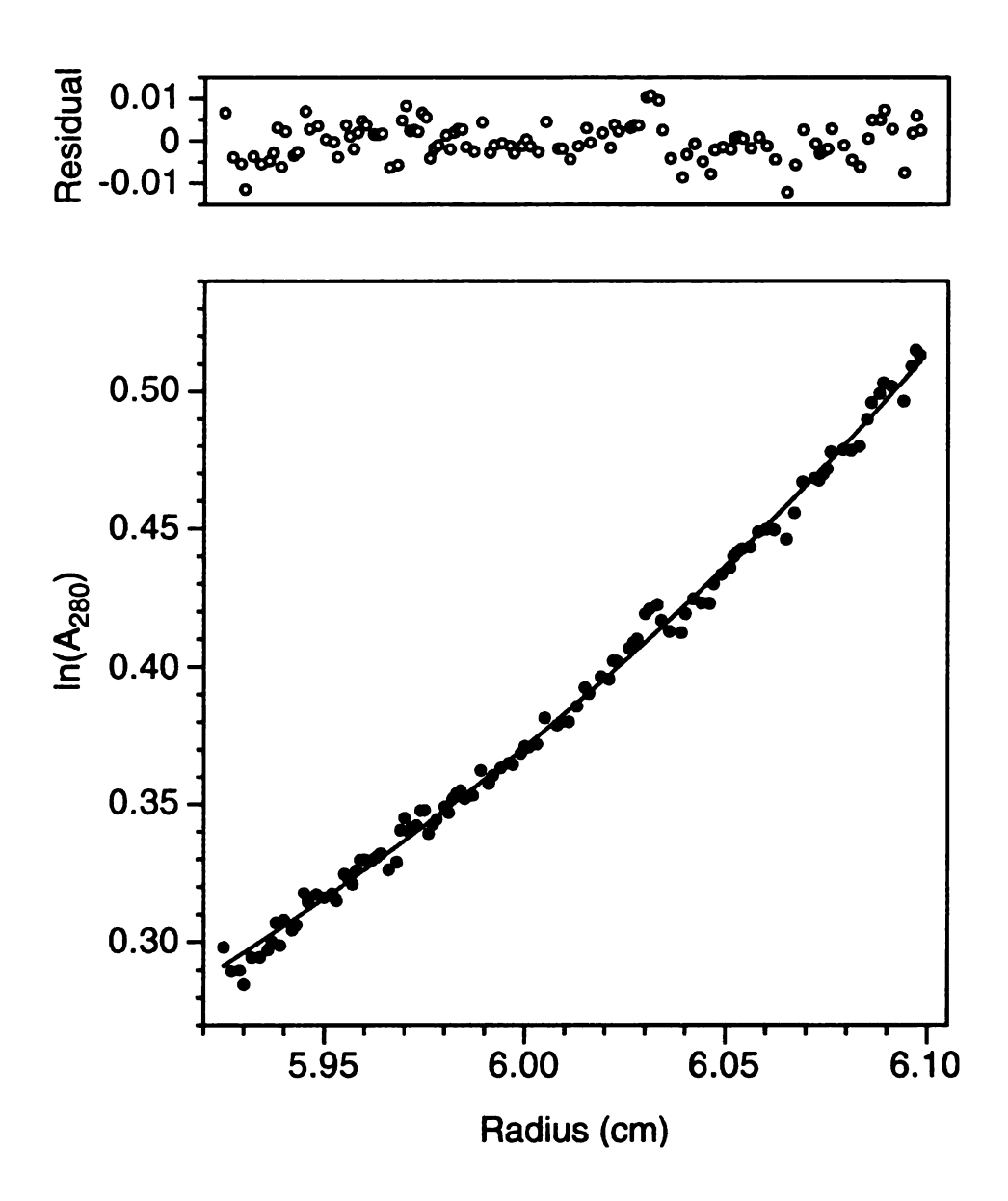


Figure 7. Equilibrium analytical ultracentrifugation data for IFP2 at 25 $^{\circ}$ C and 35,000 rpm. In the bottom panel, the experimental 280 nm absorbance is plotted vs. centrifugal radius for a 20 μ M IFP2 solution in 10 mM acetate buffer at pH 5.0. The superimposed curve represents the best-fit to the data and was obtained using a molar mass of 3900 g. The residual differences between the experimental and fitted absorbances are displayed in the top panel.

The molar mass (M) was obtained by fitting the equation:

$$(A/A_0) = \exp[M(1-V_2\rho)(r^2-r_0^2)(\omega^2/2RT)]$$
 (1)

where A_r and A₀ are the experimental absorbances at radius r and reference radius r_0 , respectively, V_2 is the partial specific volume of IFP2, ρ is the buffer density, ω is the angular velocity, R is the ideal gas constant, and T is the temperature. This equation assumes a single value of M, i.e. a single selfassociation state for all peptides in solution. The V₂ value (0.752 ml/g) was calculated from the mass average of the partial specific volumes of the individual amino acids in the peptide[10]. The value of ρ was set to 1.004 g/ml. The data displayed in Figure 7 were best-fit to M = 3900 g which is close to the monomer mass of 3300 g. As displayed in the top panel, the differences between the experimental and fitted absorbances were small and random as a function of r, which indicates that a single-species model is a reasonable. Additionally, a plot of ln(A_r) vs. r² was linear, as would be expected from Eq. (1). Fits of other data sets gave values of M between 3500 g and 4000 g. The overall result of these studies is that IFP2 at ~ 20 µM concentration is predominantly monomeric in 10 mM pH 5 acetate buffer.

Analytical ultracentrifugation studies of 80 µM IFP1 in 10 mM pH 5 acetate buffer indicated that it self-associates with a broad distribution of oligomeric states. Evidence for the presence of large oligomers included time-dependent loss of absorbance during centrifugation, which is ascribed to peptide pelleting. In addition, velocity sedimentation experiments yielded a time-dependent sedimentation coefficient. At long times, the derived sedimentation coefficient was consistent with a molar mass of ~ 10,000 g, which is about three times the monomer mass.

This suggests that while IFP1 may be comprised of oligomeric beta type structures in solution, IFP2 is monomeric in solution. Therefore, any peptide aggregation necessary to induce lipid mixing in IFP2 must occur as the peptide interacts with the lipid membrane.

2.4 Conclusions

The fusion peptide region of the HA₂ domain of the Influenza hemagglutinin protein has been the focus of considerable study because of its importance in the viral fusion process. It is necessary to show that our host-linked fusion peptides will be biologically relevant by demonstrating that they induce liposome fusion.

We have shown that the lipid mixing is induced by IFP2 in all of the lipid mixtures used in this work (Figure 5). We have also shown that lipid mixing is induced in a pH dependent way (Figure 6). This suggests that the NMR studies

detailed in this work will have some biological relevance to fusion by the fusion protein in active influenza virus.

2.5 References

- 1. Han, X., L. K. Tamm, *A host-guest system to study structure-function relationships of membrane fusion peptides.* Proceedings of the National Acadamy of Science, 2000. **97**(24): p. 13097-102.
- 2. Han, X., L. K. Tamm, *pH-dependent Self-association of Influenza Hemagglutinin Fusion Peptides in Lipid Bilayers.* Journal of Molecular Biology, 2000. **304**: p. 953-65.
- 3. Danieli, T., Sandra L. Pelletier, Yoav I. Henis, and Judith M. White, Membrane Fusion Mediated by the Influenza Virus Hemagglutinin Requires the Concerted Action of at Least Three Hemagglutinin Trimers. Journal of Cell Biology, 1996. **133**: p. 559 - 569.
- 4. Chang, C.D., et al., *Preparation and Properties of N-Alpha-9-Fluorenylmethyloxycarbonylamino Acids Bearing Tert-Butyl Side- Chain Protection.* International Journal of Peptide and Protein Research, 1980. **15**(1): p. 59-66.
- 5. Lapatsanis, L., et al., Synthesis of N-2,2,2-(Trichloroethoxycarbonyl)-L-Amino Acids and N-(9-Fluorenylmethoxycarbonyl)-L-Amino Acids Involving Succinimidoxy Anion As a Leaving Group in Amino-Acid Protection. Synthesis-Stuttgart, 1983. 8: p. 671-673.
- 6. Leray, C., Margaret Andriamampandry, Genevieve Gutbier, Jacques Cavadenti, Claudine Klein-Soyer, Christian Gachet, Jean-Pierre Cazenave, Quantitative analysis of vitamin E, cholesterol and phospholipid fatty acids in a single aliquot of human platelets and cultured endothelial cells. Journal of Chromatography B, 1997. 696: p. 33 42.
- 7. Hope, M.J., et al., Production of Large Unilamellar Vesicles By a Rapid Extrusion Procedure Characterization of Size Distribution, Trapped Volume and Ability to Maintain a Membrane-Potential. Biochimica Et Biophysica Acta, 1985. **812**(1): p. 55-65.
- 8. Struck, D.K., D. Hoekstra, and R.E. Pagano, *Use of resonance energy transfer to monitor membrane fusion*. Biochemistry, 1981. **20**(14): p. 4093-9.

- 9. Leikina, E., et al., *The 1-127 HA2 construct of influenza virus hemagglutinin induces cell-cell hemifusion.* Biochemistry, 2001. **40**(28): p. 8378-86.
- 10. Laue, T.M., et al., Computer-aided interpretation of analytical sedimentation data for proteins, in Analytical Ultracentrifugation in Biochemistry and Polymer Science, S.E. Harding, A.J. Rowe, and J.C. Horton, Editors. 1992, Royal Society of Chemistry: Cambridge. p. 90-125.

Chapter 3

Conformational Studies of Membrane and Detergent Bound Fusion Peptide by Solid State Nuclear Magnetic Resonance Rotational Echo Double Resonance Subtraction Methods

3. Conformational Studies of Membrane and Detergent Bound Fusion Peptide by Solid State Nuclear Magnetic Resonance Rotational Echo Double Resonance Subtraction Methods.

3.1 Introduction

The influenza fusion peptide has been the subject of considerable study. However, variations in sample preparation and lipid composition are common, and there are some discrepancies in the data found in the literature. In this chapter the effect of lipid composition, peptide:lipid mol ratio, and pH on the membrane bound fusion peptide structure will be studied.

Because of the low natural abundance of good NMR nuclei such as ¹³C and ¹⁵N, we generally need isotopic labeling to obtain acceptable signal-to-noise in reasonable amounts of time. With the commercial availability of amino acids isotopically enriched at specific atoms, and automated peptide synthesis, we are able to label the individual nuclei of interest in our peptides, rather than all of the nuclei in the molecule. With this 'specific' isotopic labeling, the signals resulting from the isotopically labeled nuclei will be stronger than the natural abundance signals, and will allow us to gather information on the properties of the molecule in the vicinity of the labeled nuclei. The ability to obtain residue-specific structural information makes solid-state NMR of specifically labeled peptides a powerful method for studying residue specific structure in systems that cannot be studied easily by crystallographic methods or solution NMR.

This work was done with the consensus Influenza Fusion Peptide (IFP) sequence of H-Gly-Leu-Phe-Gly-Ala-Ile-Ala-Gly-Phe-Ile-Glu-Asn-Gly-Trp-Glu-

Gly-Met-Ile-Asp-Gly-Host-NH₂, where the Host sequence consisted of either Gly-Lys-Lys-Lys (IFP1) or Gly-Gly-Lys-Lys-Lys-Lys-Trp-Lys (IFP2). Both peptides were ¹³C carbonyl labeled at Leu-2 and amide ¹⁵N labeled at Phe-3.

In NMR, information is encoded in the local field experienced by each nuclear spin in the sample. Several interactions contribute to this field. The chemical shift is the change in resonance frequency of a nuclear spin resulting from the chemical bonding environment around the nucleus. The dependence of the chemical shift on the orientation of the functional group with respect to an external magnetic field is called the chemical shift anisotropy (CSA). In addition, magnetic moments of two nuclei interact directly with one another. This interaction is the dipole-dipole coupling or dipolar coupling. The magnetic moments of two nuclei also interact with one another through chemical bonds. This interaction is spin-spin coupling or J-coupling. While J-coupling has no orientational dependence, the dipolar coupling is anisotropic and changing the orientation of the internuclear axis with respect to the externally applied magnetic field modulates this interaction.

In solution, molecules tumble rapidly, resulting in the averaging of the orientation dependent NMR interactions. This results in the observation of a sharp peak for each NMR nucleus, known as the isotropic peak. In solids, this molecular motion is greatly attenuated and the orientational dependencies remain. The local field at a nucleus is then dominated by the chemical shift anisotropy (CSA) and by the dipole-dipole coupling with nearby nuclei. These two effects result in significantly broader lines in solid-state NMR spectra than in

solution NMR. Fortunately, a technique known as magic angle spinning (MAS) improves resolution using spinning of the sample about an axis tilted at 54.7° relative to the external magnetic field[1, 2]. This spinning averages most of the CSA and dipolar coupling, and results in the much narrower isotropic peak and a series of smaller peaks separated by integral multiples of the spinning frequency from the isotropic peak. These other peaks are known as spinning sidebands. By measuring the line width and chemical shift of the isotropic peak of a labeled nucleus, we can gain insight into the structural heterogeneity and the secondary structure near this nucleus.

In this work, the peptide is synthesized with a carbonyl nucleus of interest ¹³C isotopically labeled to increase NMR sensitivity. The 23 carbonyl carbons from the remaining amino acids in the peptide contain ¹³C at ~1.1% natural abundance levels. In samples in which the peptide is associated with a lipid membrane, there are two carbonyl carbons present in each lipid head group. So, in an NMR sample with a 1:75 peptide to lipid mol ratio, if the signal from the labeled carbonyl of interest has an intensity of 1, then 0.25 units of signal arise from natural abundance carbonyl in the peptide, and 1.65 units of signal arise from natural abundance contributions from lipid head groups. Therefore, the labeled carbonyl signal accounts for only ~ 34.5% of the total signal intensity of the carbonyl region of the NMR spectrum. This large natural abundance background can make it difficult to determine the chemical shift and line width of the labeled ¹³C.

In order to observe the chemical shift of the nucleus of interest and not the signal arising from the natural abundance background in the sample, REDOR subtraction is employed[3]. In this method, a directly bonded ¹³C-¹⁵N pair is probed with ¹³C carbonyl labeling of the residue of interest and ¹⁵N amide labeling of the subsequent residue. By applying the REDOR pulse sequence[4], two spectra are obtained. The first, called the S₀ spectrum, contains signal from all of the ¹³C in the sample. In the second, called the S₁ spectrum, application of pulses which re-introduce dipolar coupling between nearby ¹³C and ¹⁵N causes attenuation of the signal of any ¹³C nucleus with a nearby (less than ~2 Å) ¹⁵N. By subtracting the S₁ data from the S₀ data, a spectrum is obtained containing only signal from ¹³C with a nearby ¹⁵N neighbor (Figure 8).

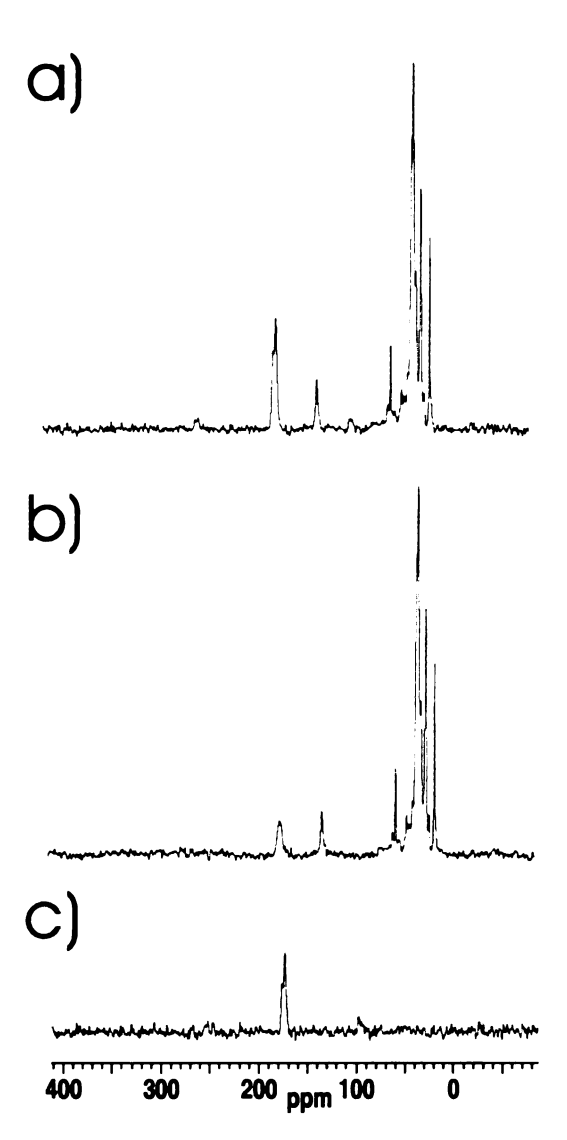


Figure 8. ¹³C solid state NMR spectra of a sample containing membrane-associated IFP2 peptide at -50 °C. The sample was prepared in 10 mM acetate buffer at pH 5.0 and with peptide:lipid mol ratio of ~ 0.014. The sample was made with POPC:POPG:Chol (8:2:5). The spectra in (a) and (b) are the respective REDOR So and So spectra. Spectrum (c) is the spectrum which results from subtracting the S₁ data from the So data. The displayed REDORfiltered difference spectrum is dominated by the Leu-2 carbonyl signal. Data were acquired with cross-polarization and with 8 kHz MAS frequency and were processed with 100 Hz Gaussian line broadening and a fifth order polynomial baseline correction. There were 41,344 S_0 and 41,344 S_1 transients.

Our solid-state NMR studies described in this section show that the structure of the Influenza fusion peptide is dependent on the lipid and cholesterol composition of the membranes with which it is associated. Lipid mixing experiments, however, show that the fusion peptide causes lipid mixing regardless of its final structure. This strongly suggests that the charge distribution and flexibility of the glycine rich influenza fusion peptide and not a

single structure are primarily responsible for the peptide's ability to disrupt, and ultimately fuse, lipid bilayer membranes.

3.2 Experimental

Materials, Peptides, and Lipid Preparation.

Materials were obtained and peptides were synthesized as outlined in Chapter 2. Preparation of large unilamellar vesicles (LUVs) was performed as described in Chapter 2.

Solid-State NMR Sample Preparation.

Samples were prepared using ~0.01% NaN₃ in either 10 mM acetate buffer at pH 5.0 or 10 mM HEPES/5 mM MES buffer at pH 7.4. A 31 ml solution containing ~.33 μmol of peptide was prepared. A 1 mL solution was then prepared which contained ~50 μmol extruded 100 nm diameter unilamellar vesicles (LUVs). This vesicle solution was added to the peptide solution and the mixture was kept at room temperature overnight to allow for peptide/lipid binding. Ultracentrifugation of the peptide/lipid mixture at 150,000g for 5 h pelleted the peptide/lipid complex and left any unbound peptide in the supernatent. However, 280 nm absorbance measurements of the supernatent indicated quantitative

binding of the peptide to the lipid. The supernatant was then decanted off and the peptide/lipid pellet formed was frozen and a portion was transferred by spatula to a magic angle spinning (MAS) NMR rotor. The total pellet volume was ~200 µl. For the room temperature experiments, the rotor was sealed with a vespel end cap that had been pre-cooled in liquid nitrogen before insertion into the rotor. This end cap fit snugly in the rotor at liquid nitrogen temperature and expanded when it warmed up so that it formed a very tight seal with the rotor, which minimized sample dehydration.

Solid-State NMR Experiments.

Measurements were made using a 9.4T spectrometer (Varian Infinity Plus, Palo Alto, CA) using a triple resonance MAS probe equipped with 6 mm diameter rotors. Spacers were placed in the rotor so that the sample was restricted to the central 2/3 of the coil length (160 μl volume) because RF homogeneity was poor at the ends of the sample rotor. The NMR detection channel was tuned to ¹³C at ~100 MHz, the decoupling channel was tuned to ¹H at ~400 MHz, and the third channel was tuned to ¹⁵N at ~40 MHz. At room temperature and at 0 °C, ¹³C cross-polarization NMR signals were attenuated, presumably due to slow motion. Because of this, the spectrum in Figure 9(a) was taken at ~80 °C, and all of the other NMR data was taken at ~50 °C with the exception of the spectra in Figure 10, which were taken at room temperature. Experiments were carried out at a spinning frequency of 8000 ± 2 Hz. NMR spectra were taken using a REDOR

filter of the ¹³C-¹⁵N dipolar interaction so that the only signal observed in the ¹³Cdetected REDOR difference spectrum was of the labeled Leu-2 carbonyl. For the low temperature experiments, application of between 1 and 2 ms of crosspolarization (CP) at ~50 kHz was followed by a 1-ms REDOR dephasing period and then signal detection. TPPM ¹H decoupling of between 65 and 70 kHz was applied during both dephasing and detection. The ¹³C transmitter frequency was set to ~160 ppm, and the ¹⁵N frequency was near the isotropic peptide amide resonance. Two REDOR sequences were used. In "REDOR1," a ~50 kHz 13 C π pulse was placed at the beginning of each rotor cycle in the dephasing period except the first cycle. For the S₁ acquisition, the dephasing period contained a 40 kHz 15 N π pulse at the middle of each rotor cycle, while the S₀ acquisition did not contain these pulses. In "REDOR2," a single ~50 kHz 13 C π pulse was placed in the middle of the dephasing time. For the S₁ acquisition, the dephasing period contained a 40 kHz 15 N π pulse at the middle and end of each rotor cycle during the dephasing period, with two exceptions. There was no $^{15}{\rm N}~\pi$ pulse during the 13 C π pulse at the center of the dephasing period, or at the end of the final rotor cycle in the dephasing period. The S₀ acquisition did not contain these 15 N π pulses. XY-8 phase cycling was used for the 15 N and 13 C π pulses[5]. During the dephasing period, pulses were not actively synchronized to the rotor phase. To achieve optimal compensation for B₀, B₁, and spinning frequency drifts, S₀ and S₁ data were acquired alternately. The recycle delay was ~1 s. In this section, all low-temperature spectra were taken using REDOR2. In the case of the room temperature experiments REDOR1 was used and cross-polarization

was not used. Instead, a 50 kHz π /2 pulse was applied directly to the ¹³C nuclei, and a 2-5 s recycle delay was used. A 2-4 ms dephasing period was used for the room temperature experiments. All chemical shifts were externally referenced to the methylene carbon resonance of adamantane (40.5 ppm).

3.3 Results and Discussion

Solid State NMR.

Figure 9 displays solid state NMR REDOR difference spectra of (a-d) IFP1 peptide and (e-g) IFP2 at a 1:150 peptide:lipid mol ratio. Both peptides were ¹³C carbonyl labeled at Leu-2 and ¹⁵N amide labeled at Phe-3 and the REDOR-filtered difference spectra only show signals from the ¹³C labeled carbonyl carbon of Leu-2. A database of experimental, reference-corrected, protein chemical shifts was compiled by Wishart, et. Chemical shifts for each amino acid nucleus for proteins with known secondary structure were collected, and an average chemical shift for each amino acid in each secondary structure was determined. For carbonyl carbons, there is a good correlation between chemical shifts and local secondary structure[6] (Table 2).

Residue Type	Coil		Helix		Beta strand		Average	
Ala	177.67	(1.57)	179.40	(1.32)	176.09	(1.51)	178.16	(1.99)
Cys	174.93	(1.89)	176.16	(1.64)	173.57	(1.64)	174.76	(2.01)
Asp	176.31	(1.34)	178.02	(1.33)	175.54	(1.57)	176.69	(1.66)
Glu	176.43	(1.36)	178.61	(1.21)	175.35	(1.40)	177.25	(1.87)
Phe	175.59	(1.60)	177.13	(1.38)	174.25	(1.63)	175.65	(1.99)
Gly	173.89	(1.42)	175.51	(1.23)	172.55	(1.58)	173.97	(1.63)
His	174.83	(1.72)	176.98	(1.29)	174.17	(1.54)	175.34	(1.94)
Ile	175.57	(1.67)	177.72	(1.29)	174.86	(1.39)	176.05	(1.90)
Lys	176.34	(1.43)	178.40	(1.46)	175.31	(1.29)	176.85	(1.89)
Leu	176.89	(1.71)	178.53	(1.30)	175.67	(1.47)	177.26	(1.91)
Met	175.35	(1.89)	177.95	(1.12)	174.83	(1.40)	176.67	(2.00)
Asn	175.08	(1.51)	176.91	(1.55)	174.64	(1.65)	175.47	(1.78)
Pro	176.89	(1.34)	178.34	(1.45)	176.18	(1.40)	177.01	(1.53)
Gln	175.90	(1.52)	177.97	(1.29)	174.88	(1.38)	176.58	(1.87)
Arg	176.02	(1.69)	178.26	(1.43)	175.14	(1.36)	176.79	(1.98)
Ser	174.49	(1.31)	175.94	(1.39)	173.55	(1.50)	174.65	(1.66)
Thr	174.70	(1.47)	175.92	(1.15)	173.66	(1.50)	174.62	(1.66)
Val	175.66	(1.47)	177.65	(1.38)	174.80	(1.39)	175.91	(1.87)
Trp	176.15	(1.14)	178.05	(1.57)	175.41	(1.66)	176.60	(1.87)
Tyr	175.39	(1.67)	177.36	(1.40)	174.54	(1.45)	175.54	(1.89)
Total number of Chemical Shifts		5258		5445		4560		16216

Table 2: Averaged ¹³C carbonyl chemical shift values (in ppm) of experimentally measured chemical shifts categorized according to secondary structural assignment and amino-acid type. (The standard deviation is given in parentheses).

The chemical shift of 177.5 ppm for Leu-2 in the IFP1 peptide in frozen DPC detergent (Figure 9(a)) is within the range of chemical shifts expected for helical structure at Leu-2. Helical structure at Leu-2 in DPC micelles is consistent with solution NMR data[7]. Figure 9(b) displays the spectrum of IFP1 peptide in POPC:POPG (4:1) membranes. The chemical shift of 177.5 ppm is identical to the shift for IFP1 in DPC micelles, suggesting that the IFP1 Leu-2 residue is also helical in POPC:POPG (4:1) membranes. In POPC:POPG:Chol

(8:2:5) the spectrum (Figure 9(c)) displays resonances at both 177.4 ppm and 174.4 ppm. This implies a mixture of both helical (177.4 ppm component) and non-helical (174.4 ppm component) structure for IFP1 in this environment at Leu-2. A chemical shift of 174.4 ppm is observed when IFP1 is bound to a membrane whose lipid composition mimics that of the cells infected by the Influenza virus, suggesting a non-helical structure for IFP1 in its native membranes. Figures 9(e-g) correspond to spectra taken of IFP2 in POPC:POPG (4:1), POPC:POPG:Chol (8:2:5), and LM, respectively. These spectra have peaks at very similar chemical shifts as those in the corresponding IFP1 cases, which shows that the same two structures are present at Leu-2 when these peptides are bound to the same membranes. Although the chemical shifts are very similar, the distribution of signal between peaks varies between spectra of the two peptides, showing that the relative population of the two structures differs.

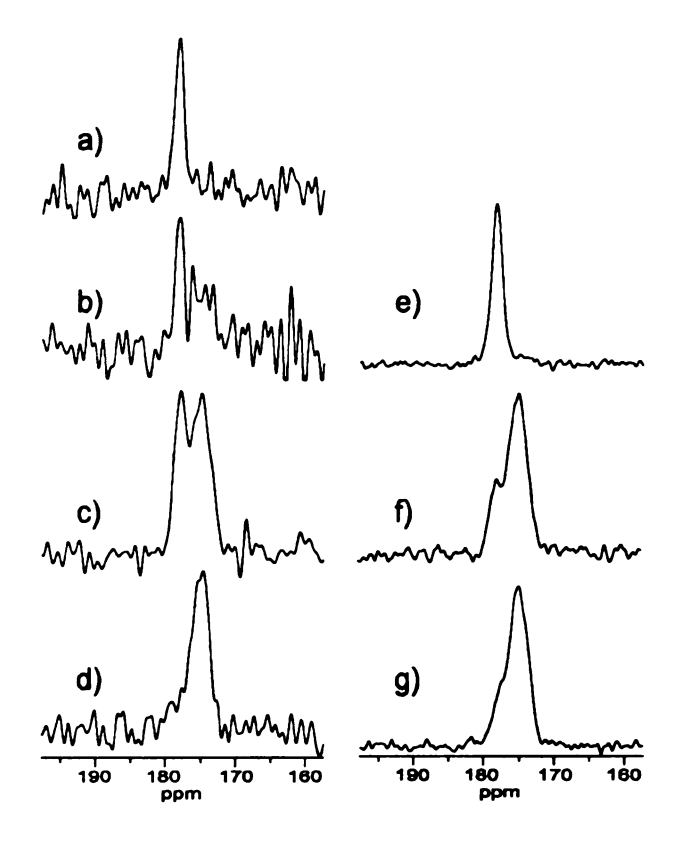


Figure 9. ¹³C solid state NMR spectra of membrane- or detergent-associated fusion peptide samples containing either (a-d) IFP1 peptide or (e-g) IFP2 peptide. Because of Leu-2 ¹³C carbonyl/Phe-3 ¹⁵N labeling of the peptides and the application of a 1.0 ms REDOR filter, the displayed REDOR difference spectra are dominated by Leu-2 carbonyl signals. For the displayed spectra, the peptide was associated with either (a) DPC detergent or the following lipid mixtures: (b, e) POPC:POPG (4:1); (c, f) POPC:POPG:Chol (8:2:5); or (d, g) LM (mixture which reflects the approximate lipid headgroup and cholesterol composition of the target epithelial cells of the virus). The (a, b, e) spectra are dominated by a peak at 177.5 ppm which indicates helical structure near Leu-2. The (d, g) spectra are dominated by a peak at 174.5 ppm which indicates non-helical structure near Leu-2. The (c. f) spectra display significant intensity at both 177.4 and 174.5 ppm which indicates a peptide population with helical structure and a peptide population with non-helical structure near Leu-2. Each sample was prepared in 10 mM acetate buffer at pH 5.0 with a peptide:lipid or peptide:detergent mol ratio of ~ 0.007. Data were acquired using crosspolarization, 8 kHz MAS frequency, and a temperature of either -80 °C (sample a) or -50 °C (samples b-g). Each spectrum was processed with 50 Hz Gaussian line broadening and fifth order polynomial baseline correction. The total $(S_0 + S_1)$ numbers of transients were: (a) 49512; (b) 253952; (c) 121344; (d) 211446; (e) 240192; (f) 286720; (g) 184320.

Figure 10 displays ¹³C NMR spectra of membrane associated influenza fusion peptide at room temperature compared to their corresponding low temperature (-50 °C) spectra. Spectrum (a) is the IFP2 peptide associated with POPC:POPG (4:1) and was taken at room temperature using the same sample as was used to for Figure 9(e). Spectrum (c) is the corresponding low temperature (-50 °C) spectrum. Spectrum (b) is the IFP1 peptide associated with POPC:POPG:Chol (8:2:5) at a peptide to lipid mol ratio of 1:75. Spectrum (d) is the spectrum of the same sample taken at –50 °C.

In Figure 10(a), the resonance at 177.8 ppm seen at room temperature is quite close to the chemical shift of 177.6 ppm observed at –50 °C. For the IFP1 peptide associated with POPC:POPG:Chol at room temperature, a broad peak is seen with a peak chemical shift and lineshape close to that of the carbonyl peak in the –50 °C case. Spectra taken of the IFP2 peptide associated with LM lipid mixture at room temperature using the same sample as was used in Figure 9(g) also suggests that the chemical shift of the Leu-2 carbonyl does not change with temperature in this membrane-bound peptide sample. These data suggest that lower temperature does not change the conformation of the influenza fusion peptide.

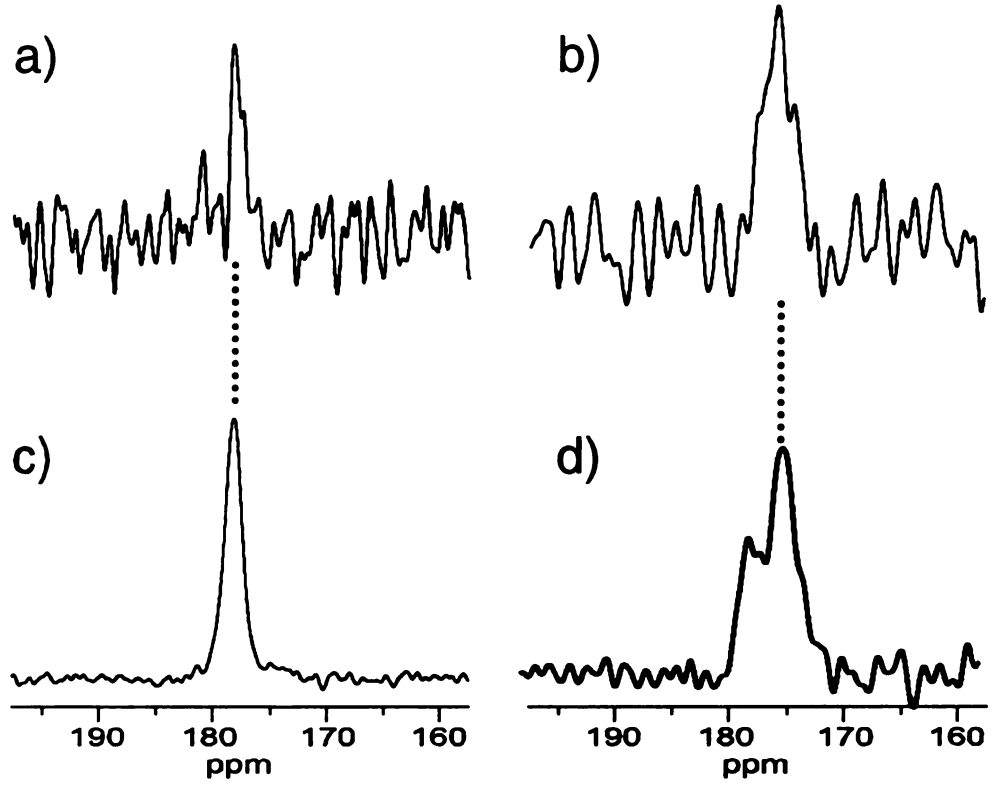


Figure 10. Room-temperature ¹³C solid state NMR spectra of membraneassociated Influenza fusion peptide compared with spectra taken at -50 °C. Spectrum (a) is the room temperature spectrum taken using the same sample as used in Figure 9(e), which contained IFP2 associated with POPC:POPG (4:1). For spectrum (b), the sample IFP1 associated with POPC:POPG:Chol (8:2:5) at a peptide to lipid ratio of ~0.14 was used. Spectra (c) and (d) are the -50 °C counterparts to spectra (a) and (b). respectively. REDOR-filtered difference spectra were taken and the observed Leu-2 carbonyl signals are displayed. Spectrum (a) has a similar chemical shift (177.8 ppm) as was observed at -50 °C, which indicates local helical structure. Spectrum (c) has a broad peak with chemical shift overlapping the chemical shifts observed in spectrum (d), suggesting that a similar mixture of structures is present at both -50 °C and at room temperature. Spectrum (a) was collected using a 5 s recycle delay and 4 ms dephasing period. Spectrum (b) was collected using a 2 s recycle delay and 2 ms dephasing period. Spectrum (a) is the result of 35008 total $(S_0 + S_1)$ transients. Spectrum (b) is the result of 80896 transients. Spectrum (c) is the result of 240192 transients, and spectrum (d) is the result of 82688 transients. Spectra (a), (c), and (d) were processed with 50 Hz Gaussian line broadening and spectrum (b) was processed with 100 Hz line broadening. All the spectra were processed using a fifth order polynomial baseline correction.

Figure 11 displays the ¹³C solid state NMR spectra of samples containing membrane-associated IFP2 peptide at –50 °C. The samples in spectra (a) and (b) were made at pH=7.4 with POPC:POPG (4:1) and with LM, respectively. The peak chemical shift of Leu-2 associated with neutral pH POPC:POPG (4:1) is 177.5 ppm, which matches the chemical shift of IFP2 peptide in POPC:POPG (4:1) membranes at pH=5.0 and suggests that the Leu-2 structure of IFP2 is not pH dependent in this environment. The peak chemical shift in spectrum (b) is 174.7 ppm and is similar to Figure 9(g), suggesting that the IFP2 peptide is non-helical when associated with the LM lipid mixture at both pH=5.0 and pH=7.4. So, the peptide structure at Leu-2 depends on lipid and cholesterol composition and is insensitive to changes in pH.

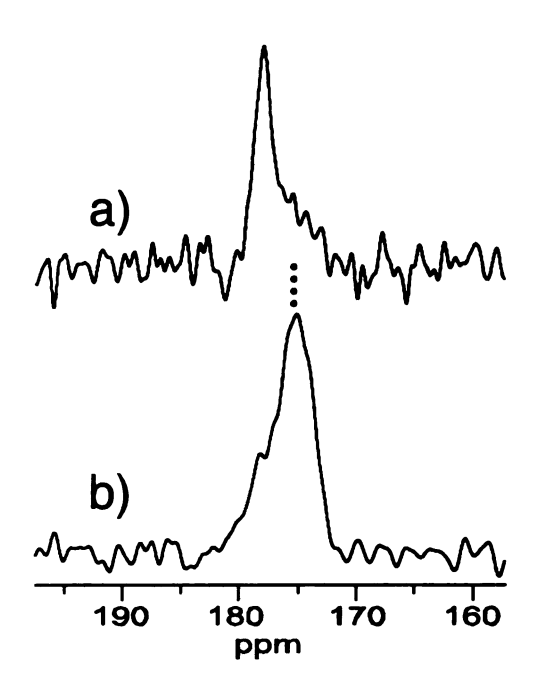


Figure 11. 13 C solid state NMR spectra of samples containing membrane-associated IFP2 peptide at -50 $^{\circ}$ C. The samples were prepared in 10 mM HEPES/5 mM MES buffer at pH 7.4 and with peptide:lipid mol ratio of \sim 0.007. The samples in spectra (a) and (b) were made with POPC:POPG (4:1) and with LM, respectively. The displayed REDOR-filtered difference spectra are dominated by Leu-2 carbonyl signals. The peak chemical shift in spectrum (a) is 177.5 ppm which indicates predominant helical structure. The peak chemical shift in spectrum (b) is 174.7 ppm which indicates predominant non-helical structure. Data were acquired with cross-polarization and with 8 kHz MAS frequency and were processed with 50 Hz Gaussian line broadening and fifth order polynomial baseline correction. For each spectrum, the total ($S_0 + S_1$) number of transients was 204800.

3.4 Conclusions

The fusion peptide region of the HA₂ domain of the Influenza hemagglutinin protein has been the focus of considerable study because of its importance in the viral fusion process. Understanding the structure of the fusion peptide will give insight into the membrane fusion process.

We have shown that the Influenza fusion peptide adopts different endstate structures when bound to lipid mixtures of different compositions. In Figure
9, we see that the fusion peptide appears to be helical in both frozen DPC
micelles and when it is associated with POPC:POPG liposomes. A mixture of
structures is observed in POPC:POPG:Chol associated fusion peptide and the
fusion peptide appears to be predominantly non-helical when bound to LM
membranes.

It appears that the introduction of cholesterol to membranes, which acts as a membrane stiffener, promotes non-helical structure in bound influenza fusion peptides.

The helical structure observed for the peptide in frozen DPC detergent is consistent with helical structure observed for the peptide in DPC detergent by solution NMR, and helical structure observed for the peptide in POPC:POPG is consistent with ESR, infrared, and circular dichroism studies in this membrane composition [7-11]. Structural plasticity in influenza and HIV fusion peptides associated with membranes has also been observed by other scientists using a variety of techniques [12-16]. Molecular dynamics studies of the influenza fusion peptide show that the peptide is very flexible, and assumes different comformations upon changes of the local environment such as pH or solvent. It is postulated that the peptide perturbs the lipid packing, which causes bilayer thinning and may facilitate membrane fusion[17]. Other fusion peptides, such as the HIV fusion peptide, and feline leukemia fusion peptide have also been shown to have considerable flexibility[15, 18].

By performing solid-state NMR measurements at both –50 °C and at room temperature (Figure 10), we have been able to show that freezing the fusion peptide sample does not change the structure of the N-terminus of the membrane bound peptide. This is important because the solid-state NMR signal-to-noise is much greater at low temperatures [19].

Solid-state NMR measurements of IFP2 associated with POPC:POPG and LM membranes at both pH=5.0, the native pH for membrane fusion, and at pH=7.4 (Figure 11) indicate that the fusion peptide adopts the same end state structure at the N-terminus at both low and neutral pH. This data agrees with other work on the fusion peptide using EPR [8] and solution NMR [20].

It was also shown in chapter two that IFP2 catalyzes lipid mixing in vesicles in which its end state structure at Leu-2 is helical, as well as in vesicles in which its end state structure at Leu-2 is non-helical (Figure 10(a)). This lipid mixing was shown to be induced by IFP2 in a pH dependent way (Figure 6). Because both final structures of the fusion peptide can induce lipid mixing in a pH dependent way, it seems that both peptide structures can catalyze membrane fusion. This may mean that the structure of the fusion peptide is not important to fusogenicity, or that there are two or more fusion active structures for the peptide. Because membrane fusion is a rapid, multi-step process, structural information is available only on equilibrium products of the fusion process. Since we only observe final peptide conformations and none of the intermediate changes adopted at various stages of the fusion process, it is possible that disruption of

the membrane bilayer, and structural flexibility will be key to the function of the fusion peptide.

We have shown that, in lipid mixtures in which the peptide is helical at neutral pH, such as POPC:POPG, the end structure of the fusion peptide is also helical at low pH after lipid mixing has occurred. Similarly, in environments where the fusion peptide is non-helical prior to fusion, such as in the LM lipid mixture, we see non-helical structure persist after lipid mixing. This shows that the influenza fusion peptide induces lipid mixing when it has one of two distinct membrane associated structures. This is the first evidence that I have been able to find of two different fusion peptide structures promoting membrane fusion.

Because a single final peptide structure has not been implicated in the fusion process, I am swayed by fusion peptide models in which one specific structure of the peptide is not critical. The peptide might disrupt one or both bilayers and then act as a space filler between the hydrophobic lipid tails, shielding acyl chains from water to stabilize the perturbed membranes and to promote membrane fusion [21].

3.5 References

- 1. Slichter, C.P., *Principles of Magnetic Resonance*. 3 ed. 1996, New York: Springer. 655.
- 2. Schmidt-Rohr, K. and H.W. Spiess, *Multidimensional Solid-State NMR and Polymers*. 1994, San Diego: Academic Press.
- 3. Yang, J., et al., Application of REDOR Subtraction for Filtered MAS Observation of Labeled Backbone Carbons of Membrane-Bound Fusion Peptides. Journal of Magnetic Resonance, 2002. **159**(2): p. 101-110.
- 4. Gullion, T., *Introduction to rotational-echo, double-resonance NMR.* Concepts in Magnetic Resonance, 1998. **10**(5): p. 277-289.
- 5. Gullion, T., D.B. Baker, and M.S. Conradi, *New, Compensated Carr-Purcell Sequences*. Journal of Magnetic Resonance, 1990. **89**(3): p. 479-484.
- 6. Zhang, H., Stephen Neal, and David S. Wishart, *RefDB: A database of uniformly referenced protein chemical shifts.* Journal of Biomolecular NMR, 2003. **25**: p. 173-195.
- 7. Han, X., Bushweller, J. H., Cafiso, D. S., Tamm, L. K., *Membrane structure and fusion-triggering conformational change of the fusion domain from influenza hemagglutinin.* Nat Struct Biol, 2001. **8**(8): p. 715-20.
- 8. Macosko, J.C., C.H. Kim, and Y.K. Shin, *The membrane topology of the fusion peptide region of influenza hemagglutinin determined by spin-labeling EPR.* J Mol Biol, 1997. **267**(5): p. 1139-48.
- 9. Han, X. and L.K. Tamm, *A host-guest system to study structure-function relationships of membrane fusion peptides.* Proceedings of the National Academy of Sciences of the United States of America, 2000. **97**(24): p. 13097-13102.
- 10. Dubovskii, P.V., et al., *Structure of an analog of fusion peptide from hemagglutinin*. Protein Science, 2000. **9**(4): p. 786-798.

- 11. Hsu, C.H., et al., Structural characterizations of fusion peptide analogs of influenza virus hemagglutinin Implication of the necessity of a helix-hinge-helix motif in fusion activity. Journal of Biological Chemistry, 2002. 277(25): p. 22725-22733.
- 12. Han, X., Tamm, L. K., pH-dependent self-association of influenza hemagglutinin fusion peptides in lipid bilayers. J Mol Biol, 2000. **304**(5): p. 953-65.
- 13. Durell, S.R., et al., What studies of fusion peptides tell us about viral envelope glycoprotein-mediated membrane fusion (review). Mol Membr Biol, 1997. **14**(3): p. 97-112.
- 14. Martin, I., et al., Lipid membrane fusion induced by the human immunodeficiency virus type 1 gp41 N-terminal extremity is determined by its orientation in the lipid bilayer. J Virol, 1996. **70**(1): p. 298-304.
- 15. Davies, S.M.A., et al., Structural plasticity of the feline leukaemia virus fusion peptide: a circular dichroism study. Febs Letters, 1998. **425**(3): p. 415-418.
- 16. Saez-Cirion, A. and J.L. Nieva, *Conformational transitions of membrane-bound HIV-1 fusion peptide*. Biochimica Et Biophysica Acta-Biomembranes, 2002. **1564**(1): p. 57-65.
- 17. Vaccaro, L., K. J. Cross, J. Kleinjung, S. K. Straus, D. J. Thomas, S. A. Wharton, J. J. Skehel, and F. Fraternali, *Plasticity of Influenza Haemagglutinin Fusion Peptides and Their Interaction with Lipid Bilayers*. Biophysical Journal, 2005. **88**: p. 25 36.
- 18. Asier Saez-Cirion, J.L.N., *Conformational Transitions of Membrane-Bound HIV-1 Fusion Peptide*. Biochemica et Biophysica Acta, 2002. **1564**: p. 57 65.
- 19. Bodner, M.L., et al., Temperature Dependence and Resonance Assignment of 13C NMR Spectra of Selectively and Uniformly Labeled Fusion Peptides Associated with Membranes. Magnetic Resonance in Chemistry, 2004. **42**: p. 187 194.

- 20. Zhou, Z., J. C. Macosko, D. W. Hughes, B. G. Sayer, J. Hawes, and R. M. Epand, ¹⁵N NMR Study of the Ionization Properties of the Influenza Virus Fusion Peptide in Zwitterionic Phospholipid Dispersions. Biophysical Journal, 2000. **78**: p. 2418-25.
- 21. Bentz, J., *Membrane Fusion Mediated by Coiled Coils: A Hypothesis*. Biophysical Journal, 2000. **78**: p. 886-900.

Chapter 4

Solid State Nuclear Magnetic Resonance Rotational Echo Double Resonance Measurements to Probe for a pH Dependent Structural Feature in the Fusion Peptide

4. Solid State Nuclear Magnetic Resonance Rotational Echo Double Resonance Measurements to Probe for a pH Dependent Structural Feature in the Fusion Peptide.

4.1 Introduction

The significance of the fusion peptide in influenza viral fusion is suggested from atomic-resolution structures of influenza fusion protein domains. The crystal structure for the influenza hemagglutinin fusion protein exists both at nonfusogenic pH 7[1] and at fusogenic pH 5[2, 3], although the fusion peptide domain was deleted from the constructs used in the latter structures. These structures provide evidence for a major conformational change in the influenza hemagglutinin protein which moves the fusion peptide ~100 Å relative to the rest of the molecule[4]. This conformational change results in the movement of the fusion peptide from the inside of the protein to the exterior so that it can interact with target cell and possibly viral membranes. Analysis of these structures and consideration of other fusion data have led to at least four proposed models of influenza/endosome fusion[2, 4-7]. In each of these models, insertion of the fusion peptide and bilayer disruption play an integral role in membrane fusion.

Although the influenza fusion peptide has been studied extensively, there is some variation between proposed fusion peptide structures. Some groups have observed helical structure at low pH for the peptide in DPC detergent solution by NMR and for the peptide in POPC:POPG membranes by ESR, IR, and circular dichroism[8-12]. While some groups report no change in helix

orientation and no apparent structural change between high and low pH structures by EPR [9, 13] other groups have proposed considerable structural changes in the fusion peptide between low and high pH[8, 14]. The work in this chapter probes pH dependent structural change.

Figure 12 displays a solution NMR structure of the fusion peptide in DPC micelles that suggests that the peptide takes on a low pH structure characterized by an N-terminal helix, followed by a short turn, followed by a 3₁₀ helix at low pH and takes on a neutral pH structure characterized by an N-terminal helix followed by a random coil [8]. Infrared, circular dichroism (CD), and electron spin resonance (ESR) data are most consistent with a 'tilted helix' structural model for the interaction of the fusion peptide with the membrane[9, 15]. In this model, the peptide helix makes an oblique angle of approximately 65° with respect to the membrane bilayer normal [9, 16].

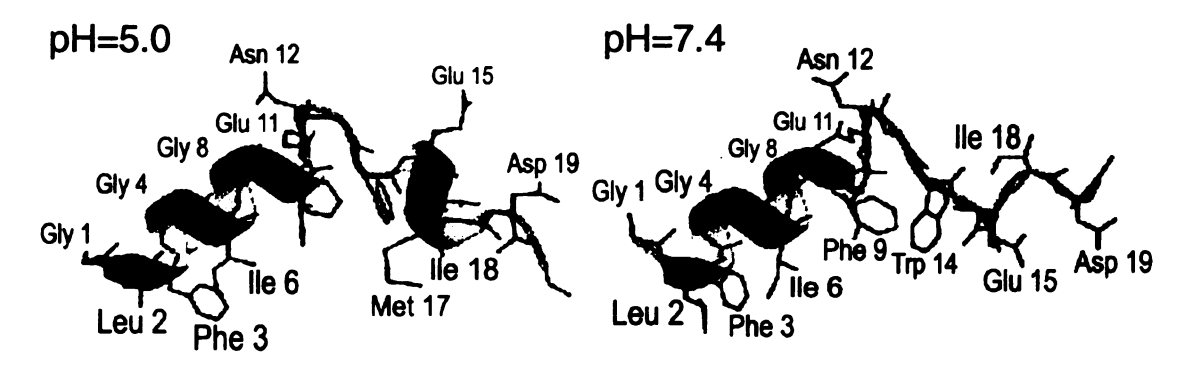


Figure 12. Solution NMR structure of the influenza fusion peptide in DPC micelles showing an N-terminal alpha helix followed by a bend and a short 3₁₀ helix at low pH. The 3₁₀ helix is absent at neutral pH in this structure.

In this chapter REDOR will be used test for the presence of the 3₁₀ helix proposed to be absent at neutral pH and present at low pH. REDOR recoupling reintroduces heteronuclear dipolar couplings between nearby ¹³C and ¹⁵N nuclei under magic angle spinning. The dipolar coupling has a 1/r³ dependence on ¹³C – ¹⁵N distance, and will cause signal attenuation in NMR spectra, so measurement of the ¹³C attenuation after various periods of REDOR recoupling will allow determination of the distance between a labeled ¹³C and ¹⁵N[17, 18]. For this work, peptides with a ¹³C carbonyl at Gly-13 and an ¹⁵N amide nitrogen at Gly-16 were used. If a 3₁₀ helix is present across these residues, then they will be linked by a hydrogen bond and these two nuclei will be separated by a distance of ~4 Å. This distance would be considerably greater in a random coil.

Our work demonstrates that the 3₁₀ helix is present in influenza fusion peptide at both low and at neutral pH when the peptide is associated with DPC micelles or with bilayer lipid membranes consisting of 1-palmitoyl-2-oleoyl-sn-

glycero-3-phosphocholine (POPC) and 1-palmitoyl-2-oleoyl-sn-glycero-3-[phospho-rac-(1-glycerol)] (POPG).

4.2 Experimental

Materials, Peptides, and Lipid Preparation.

Materials were obtained as outlined in Chapter 2. Preparation of large unilamellar vesicles (LUVs) was performed as described in Chapter 2.

A 17 residue peptide (sequence AEAAAKEAAAKEAAAKA) (I4) that is predominantly α -helical when lyophilized was synthesized as a C-terminal amide with 13 C carbonyl labeling at Ala-9 and 15 N amide labeling at Ala-13. When lyophilized these two labeled nuclei should have a C-N internuclear distance of \sim 4.1 Å[19].

The fusion peptide was synthesized with the 20 N-terminal residues of the Influenza A hemagglutinin fusion protein (sequence GLFGAIAGFIENGWEGMIDG) followed by a lysine rich 'host sequence' to improve aqueous solubility[20]. This sequence was GGKKKKWKWK (IFP2). The tryptophans were added to improve UV quantitation. The peptide was synthesized as its C-terminal amide using a peptide synthesizer (ABI 431A, Foster City, CA) equipped for FMOC chemistry and was ¹³C carbonyl labeled at Gly-13 and amide ¹⁵N labeled at Gly-16.

Solid-State NMR Sample Preparation.

Lipid samples were prepared as described in Chapter 3.

The detergent sample was made by addition of 160 µL 200 mM DPC in 10 mM HEPES/5 mM MES buffer at pH 7.4 to 0.53 µmol lyophilized IFP. At the conclusion of the pH 7.4 experiments the pH of this sample was adjusted to 5.0 using 1.0 M citric acid. The amount of acid required was determined experimentally by adjusting the pH of a series of detergent solutions. NMR experiments were then carried out at pH 5.0.

Solid-State NMR Experiments.

At room temperature and at 0 °C, ¹³C cross-polarization NMR signals were attenuated, presumably due to slow motion. In order to obtain signal in a reasonable period of time, all of the NMR data was taken at –50 °C, except for the detergent spectra. Because of greater motion present in the detergent micelle samples, these spectra were taken at –80 °C. All spectra in this section were acquired using REDOR1. The recycle delay was 1.0 s for the lipid samples and 2.0 s for the detergent samples. All other experimental parameters were the same as described in Chapter 3.

REDOR Data Analysis.

In these experiments, the difference between S_0 and S_1 signal intensity is referred to as "dephasing" and the (dephasing)/(S_0 signal intensity) is referred to as the "fractional dephasing." For each pair of S_0 and S_1 spectra, the S_1 data points were subtracted from the S_0 data points and the resulting spectrum was used to determine the peak chemical shift of the dephased peak. The integrated intensity of a 1 ppm region about this peak chemical shift value was used to determine S_0 and S_1 intensity for calculation of the fractional dephasing. For each pair of S_0 and S_1 spectra, an experimental uncertainty (σ) was calculated as the root mean squared deviation of integrated intensities in 22 1 ppm regions of the spectra without signal. The uncertainty in the fractional dephasing was calculated using the formula [21]:

$$\sigma_{\text{Fractional Dephasing}} = \sigma(S_1/S_0)[(1/S_0)^2 + (1/S_1)^2]^{1/2}$$

4.3 Results and Discussion

Solid State NMR.

Figure 13 displays solid state NMR REDOR spectra of the lyophilized helical I4 peptide isotopically labeled with a 13 C carbonyl label at Ala-9 and 15 N amide nitrogen label at Ala-13. These two nuclei should have a C-N internuclear distance of ~4.1 Å due to the hydrogen bond present between the residues in the α -helix. Table 3 gives the fractional dephasing as a function of dephasing time.

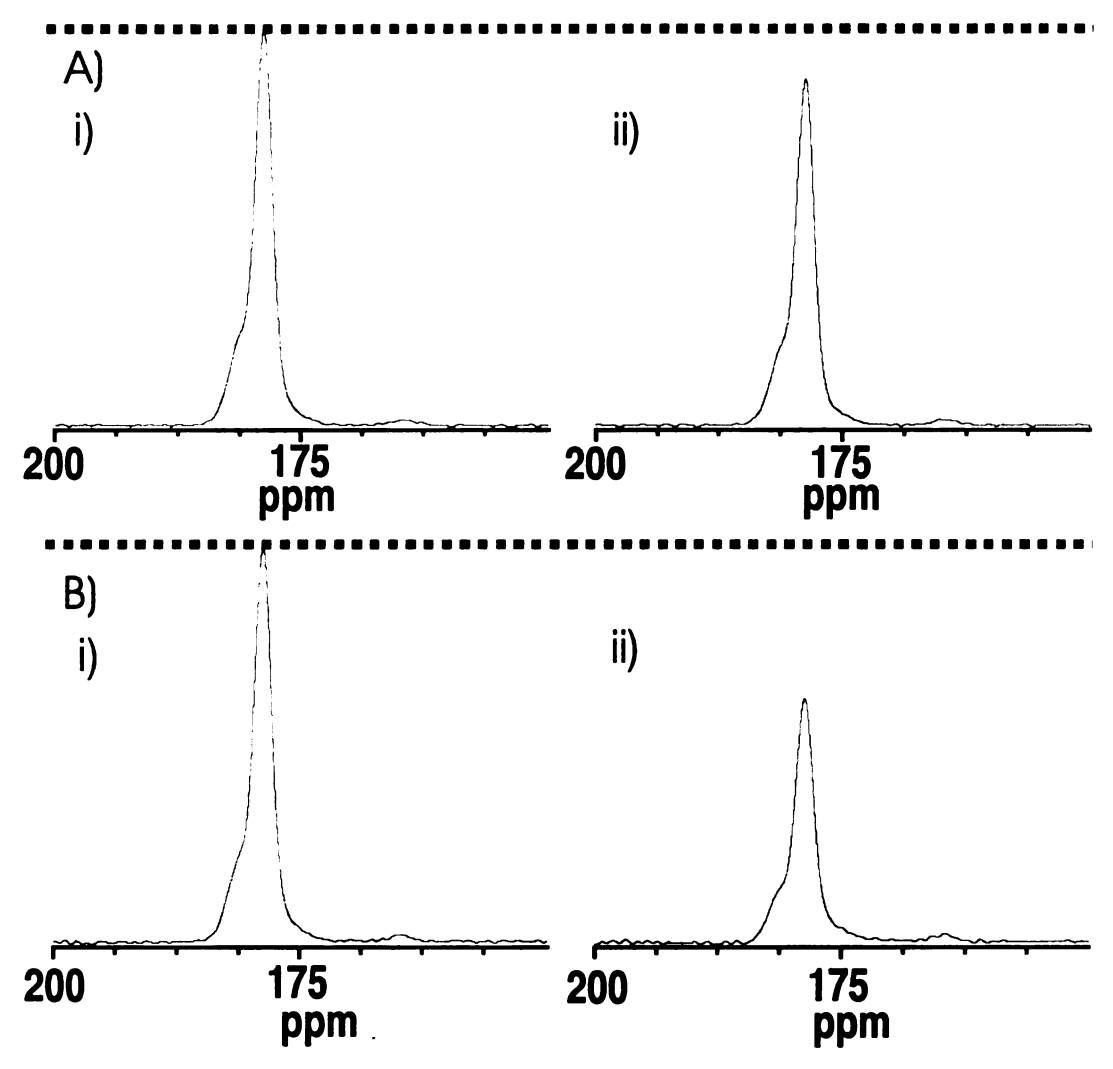


Figure 13. 13 C solid state NMR spectra of lyophilized I4 peptide taken at -50 $^{\circ}$ C. Spectra (a) were taken using an 8 ms REDOR dephasing period. Spectra (b) were taken using a 16 ms dephasing period. The S_0 spectra are denoted (i) while the S_1 spectra are marked (ii). In this system, the structure is known and the 13 C carbonyl and 15 N amide labels have been placed on two residues known to be connected by a hydrogen bond in an α -helix. The considerable dephasing confirms the close proximity of the isotopic labels in this system. Each spectrum is the result of 512 transients.

These data give us a good reference for the amount of dephasing to be expected between the carbonyl carbon and amide nitrogen of two hydrogen bonded amino acids in a peptide. These numbers are similar to the data obtained for IFP both in DPC micelles and in lipid bilayers at both pH 5.0 and 7.4 and support a model in which Gly-13 and Gly-16 in IFP are connected by a hydrogen bond in these environments, as they would be in a 3₁₀ helical conformation. These results are summarized in Table 3.

Sample	Experimental Fractional Dephasing
DPC pH 5 16 ms	0.41 (.08)
DPC pH 7 16 ms	0.30 (.14)
POPC:POPG pH 5 8 ms	0.18 (.05)
POPC:POPG pH 5 16 ms	0.33 (.09)
POPC:POPG pH 7 8 ms	0.15 (.03)
POPC:POPG pH 7 16 ms	0.29 (.07)
I4 Peptide 8 ms	0.127 (.002)
I4 Peptide 16 ms	0.386 (.002)

Table 3. Summary of REDOR results. Considerable dephasing in DPC micelles and POPC:POPG (4:1) lipid membranes at both pH 7.4 and pH 5.0 suggests the presence of a 3₁₀ helix in the fusion peptide in both environments at both pH's. The numbers in parentheses are the uncertainties in the experimental dephasing.

Figure 14 displays solid state NMR REDOR spectra of IFP in DPC micelles at ~0.014 peptide:detergent mol ratio. The considerable dephasing of the Gly-13 carbonyl suggests close proximity to the Gly-16 amide nitrogen. It appears that the 3₁₀ helix suggested by solution NMR studies of these peptides in DPC micelles is present at both pH 5.0 and pH 7.4[8].

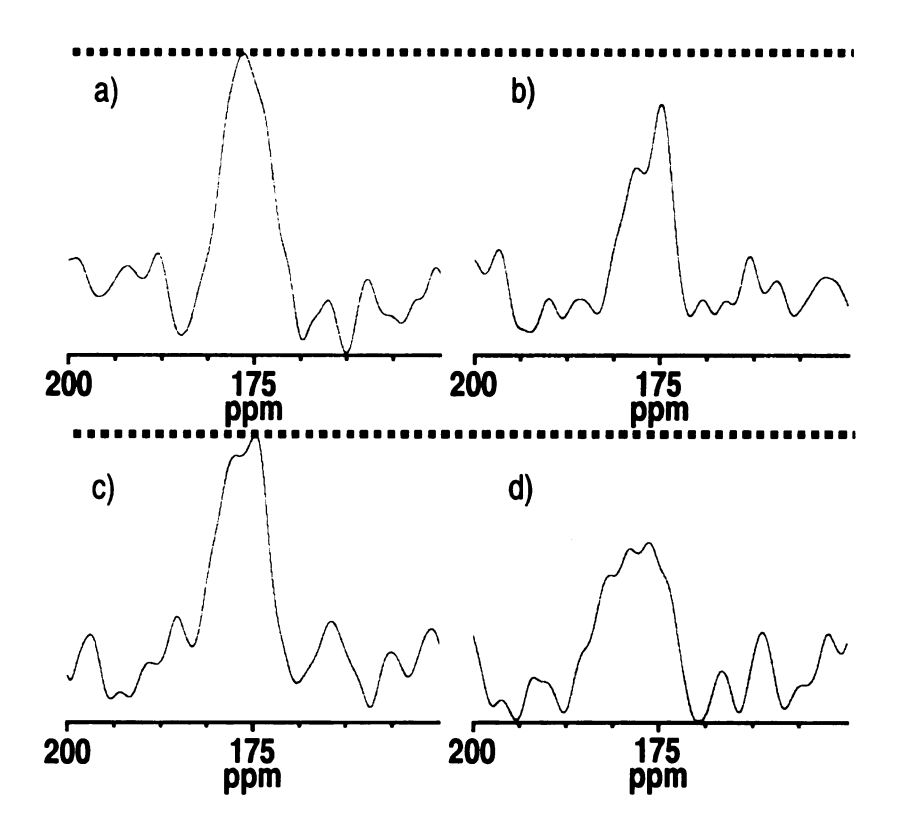


Figure 14. ¹³C solid state NMR REDOR spectra of detergent-associated fusion peptide samples with a peptide:detergent ratio of .014 at pH 7.4 and pH 5.0. Because of Gly-13 ¹³C carbonyl/Gly-16 ¹⁵N labeling of the peptide the majority of the dephasing is the result of the dipolar coupling between Gly-13 and Gly-16. Spectra (a) and (c) are the S₀ spectra for IFP associated with DPC micelles at pH 7.4 and pH 5.0 respectively. Spectra (b) and (d) are the corresponding S₁ spectra. These spectra were taken with a 16 ms REDOR dephasing period. The considerable dephasing present in both spectra indicates strong dipolar coupling between Gly-13 and Gly-16, which is indicative of a hydrogen bond present in a 3₁₀ helix. The spectra were processed with 250 Hz Gaussian line broadening and fifth order polynomial baseline correction. Spectra (a) and (b) are each the result of 198208 transients and spectra (c) and (d) are each the result of 277496 transients.

Figure 15 displays solid state NMR REDOR spectra of IFP associated with POPC:POPG (4:1) lipid membranes at pH 5.0. Because the peptide was ¹³C carbonyl labeled at Gly-13 and ¹⁵N amide labeled at Gly-16 the considerable dephasing of the Gly-13 carbonyl suggests close proximity to the Gly-16 amide nitrogen. Table 3 gives the fractional dephasing as a function of dephasing time.

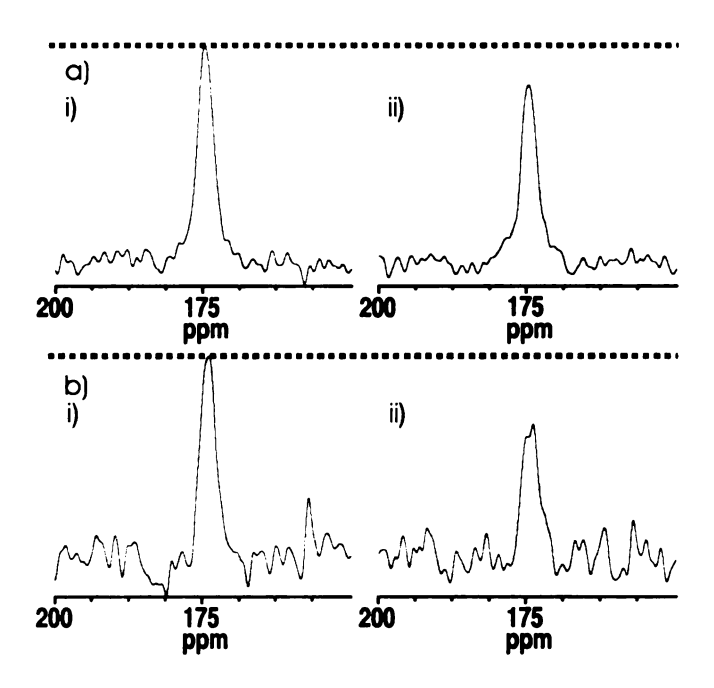


Figure 15. ¹³C solid state NMR spectra of membrane-associated IFP taken at -50 °C at pH 5.0. Spectrum (a) is the spectrum taken using an 8 ms REDOR dephasing period. Spectrum (b) is the spectrum resulting from a 16 ms dephasing period. The (i) spectra are the S₀ spectra and the spectra denoted by (ii) are the corresponding S₁ spectra. The considerable dephasing present is indicative of close proximity of the ¹³C labeled carbonyl at Gly-13 and the ¹⁵N labeled amide nitrogen at Gly-16. All of the spectra were processed with 100 Hz Gaussian line broadening and fifth order polynomial baseline correction. The (a) spectra are the result of 40960 S₀ and S₁ transients and the (b) spectra are the result of 112640 S₀ and S₁ transients.

Figure 16 displays solid state NMR REDOR spectra of IFP associated with POPC:POPG (4:1) lipid membranes at pH 7.4. Table 3 gives the fractional dephasing as a function of dephasing time. Because the peptide was ¹³C carbonyl labeled at Gly-13 and ¹⁵N amide labeled at Gly-16 the considerable dephasing of the Gly-13 carbonyl suggests close proximity to the Gly-16 amide nitrogen. This reinforces the idea that the 3₁₀ helix is present at both pH 5.0 and pH 7.4.

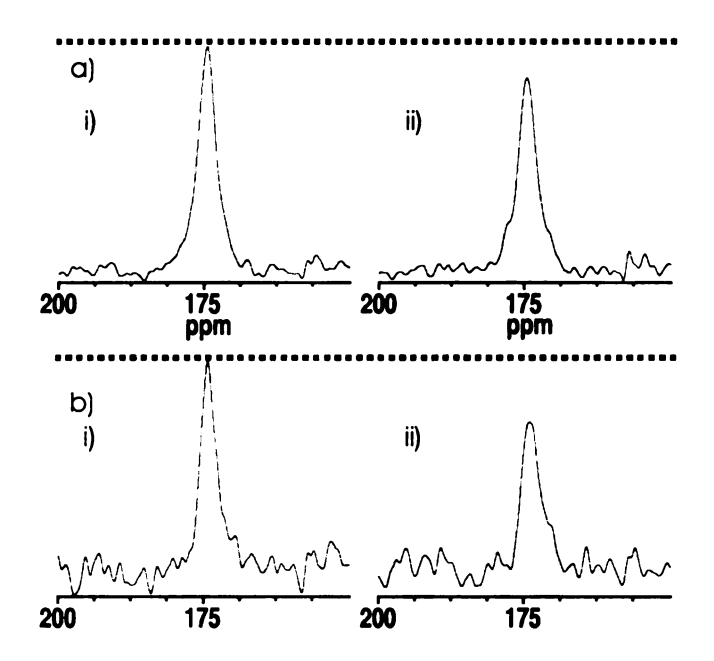


Figure 16. 13 C solid state NMR spectra of membrane-associated IFP at -50 $^{\circ}$ C at pH 7.4. Spectra (a) were taken using an 8 ms REDOR dephasing period. Spectra (b) were taken using a 16 ms dephasing period. As in the pH 5.0 cases, the S₀ spectra are denoted (i) while the S₁ spectra are marked (ii). Again, the considerable dephasing suggests close proximity between the isotopic labels at the Gly-13 carbonyl carbon and the Gly-16 amide nitrogen. All of the spectra were processed with 100 Hz Gaussian line broadening and a seventh order polynomial baseline correction. The (a) spectra are the result of 122880 S₀ and S₁ transients and the (b) spectra are the result of 256000 S₀ and S₁ transients.

Figure 17 displays solid state NMR REDOR subtraction spectra of IFP associated with POPC:POPG (4:1) lipid membranes at pH 5.0 and pH 7.4. These spectra are differences between the S_0 and S_1 data in Figures 15(a) and 16(a) respectively. These difference spectra are dominated by the 13 C carbonyl of Gly-13. At pH 5.0 the Gly-13 carbonyl peak shift is at 174.8 ppm and the full-width at half-maximum (FWHM) is approximately 330 Hz. At pH 7.4 the Gly-13 carbonyl resonates at 174.4 ppm and has a FWHM of about 265 Hz. The average chemical shift of a glycine carbonyl in a helical conformation has been shown to be 175.51 \pm 1.23 ppm while a glycine in a beta sheet structure has a chemical shift of 172.55 \pm 1.58[22]. The agreement between the Gly-13 chemical shift values at both pHs and the average helical shift lends credence to the hypothesis that the Gly-13 region of the fusion peptide is in a helical conformation at both pHs.

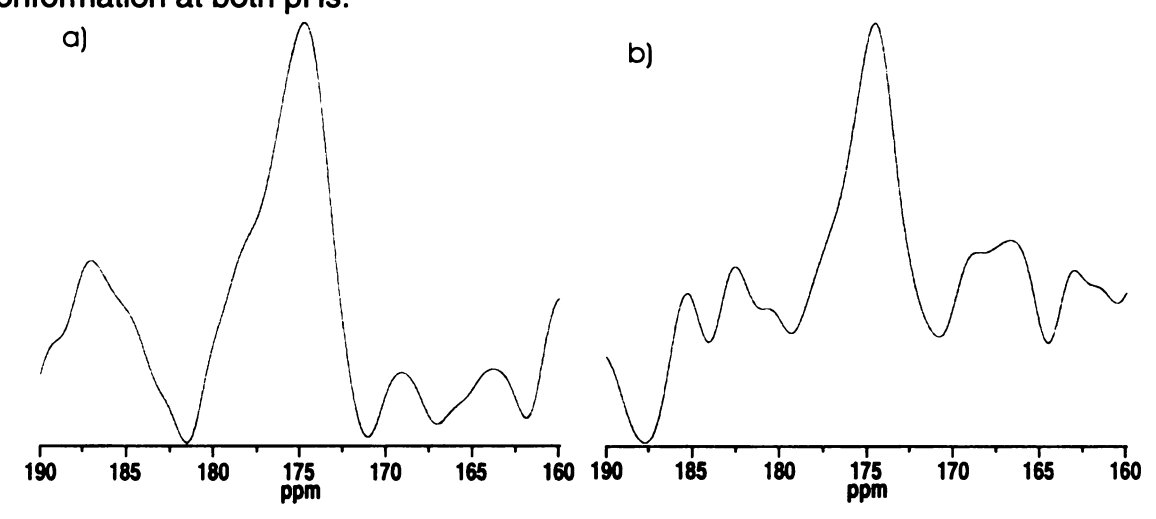


Figure 17. 13 C solid state NMR REDOR difference spectra of membrane-associated IFP taken at -50 °C with 8 ms of dephasing. The spectra in (a) and (b) result from the subtraction of the S_1 data from the S_0 data from Figure 15(a) and Figure 16(a) respectively. Both spectra were processed with 100 Hz Gaussian line broadening and a seventh order polynomial baseline correction.

Despite considerable study there is some discrepancy in the proposed structures for the influenza fusion peptide. In our study, the helical structure observed for the peptide in frozen DPC detergent at pH 5.0 is consistent with helical structure observed for the peptide in DPC detergent by solution NMR and with helical structure observed for the peptide in POPC:POPG by ESR, infrared, and circular dichroism[8, 9, 11, 12, 23]. Some groups report no change in helix orientation with respect to the membrane normal, and no apparent structural change between high pH and low pH structures as determined by EPR [9, 13]. Other work suggests a considerable structural change in the fusion peptide C-terminus between low and high pH [8, 14]. The solution NMR structure published for the fusion peptide in POPC:POPG shows an N-terminal helix, followed by a short turn, followed by a 3₁₀ helix present at low pH but absent at neutral pH (See Figure 12)[8].

Solid-state NMR REDOR measurements of the fusion peptide in frozen DPC micelles at both pH 5.0 and pH 7.4 (Figure 14) and in lipid bilayers at both neutral and low pH (Figure 16 and 15), support a large population of 3₁₀ helix between Gly-13 and Gly-16 present at both pH 5.0 and pH 7.4. This conclusion is supported by the fact that the chemical shift, which is a sensitive probe of local environment, is similar in the POPC:POPG samples at both pHs (Figure 17). This suggests a re-examination of models for the pH-dependence of IFP bilayer fusion based on the formation of a C-terminal 3₁₀ helix at low pH and a coil structure at neutral pH. One explanation for the failure to detect a 3₁₀ helix in the DPC bound fusion peptide at neutral pH by solution NMR could be the

attenuation of NOE's used to constrain the structure because of higher rates of amide proton exchange at high pH.

One could argue that freezing might distort the samples used in our studies. We see no significant temperature dependence of chemical shifts between room temperature and -50°C (Figure 10), which suggests that freezing these samples causes no significant changes in structure.

Our data lead us to conclude that the 3₁₀ helix illustrated by the low pH solution NMR structure is also present at neutral pH. Because we see no evidence for a significant pH-induced structural change in the fusion peptide, I feel that any model which relies on the formation of this structural feature warrants reexamination.

We have also shown in Chapter 3 that at least two distinct fusion peptide structures can induce lipid mixing. Because of the flexibility of the fusion peptide, a transient structure or some conformational flip-flop of the peptide may be important for inducing fusion. I believe that the fusion peptide may act as a space filler between the hydrophobic lipid tails to stabilize the perturbed membranes and to catalyze membrane fusion[5, 24].

4.4 References

- 1. Wilson, I.A., J.J. Skehel, and D.C. Wiley, *Structure of the haemagglutinin membrane glycoprotein of influenza virus at 3 A resolution*. Nature, 1981. **289**(5796): p. 366-73.
- 2. Bullough, P.A., et al., *Structure of influenza haemagglutinin at the pH of membrane fusion*. Nature, 1994. **371**(6492): p. 37-43.
- 3. Chen, J., J. J. Skehel, and D. C. Wiley, *N- and C-terminal residues combine in the fusion-pH influenza hemagglutinin HA*₂ subunit to form an *N cap that terminates the triple-stranded coiled coil.* Porceedings of the National Acadamy of Science of the United States of America, 1999. **96**: p. 8967-72.
- 4. Carr, C.M. and P.S. Kim, *A spring-loaded mechanism for the conformational change of influenza hemagglutinin.* Cell, 1993. **73**(4): p. 823-32.
- 5. Bentz, J., *Membrane fusion mediated by coiled coils: a hypothesis.* Biophys J, 2000. **78**(2): p. 886-900.
- 6. Kozlov, M.M. and L.V. Chernomordik, *A mechanism of protein-mediated fusion: coupling between refolding of the influenza hemagglutinin and lipid rearrangements.* Biophys J, 1998. **75**(3): p. 1384-96.
- 7. Bonnafous, P. and T. Stegmann, *Membrane perturbation and fusion pore formation in influenza hemagglutinin-mediated membrane fusion. A new model for fusion.* J Biol Chem, 2000. **275**(9): p. 6160-6.
- 8. Han, X., Bushweller, J. H., Cafiso, D. S., Tamm, L. K., *Membrane* structure and fusion-triggering conformational change of the fusion domain from influenza hemagglutinin. Nat Struct Biol, 2001. **8**(8): p. 715-20.
- 9. Macosko, J.C., C.H. Kim, and Y.K. Shin, *The membrane topology of the fusion peptide region of influenza hemagglutinin determined by spin-labeling EPR*. J Mol Biol, 1997. **267**(5): p. 1139-48.

- 10. Han, X., Tamm, L. K., pH-dependent self-association of influenza hemagglutinin fusion peptides in lipid bilayers. J Mol Biol, 2000. **304**(5): p. 953-65.
- 11. Hsu, C.H., et al., Structural characterizations of fusion peptide analogs of influenza virus hemagglutinin Implication of the necessity of a helix-hinge-helix motif in fusion activity. Journal of Biological Chemistry, 2002. 277(25): p. 22725-22733.
- 12. Dubovskii, P.V., et al., *Structure of an analog of fusion peptide from hemagglutinin*. Protein Science, 2000. **9**(4): p. 786-798.
- 13. Zhou, Z., J. C. Macosko, D. W. Hughes, B. G. Sayer, J. Hawes, and R. M. Epand, ¹⁵N NMR Study of the Ionization Properties of the Influenza Virus Fusion Peptide in Zwitterionic Phospholipid Dispersions. Biophysical Journal, 2000. **78**: p. 2418-25.
- 14. Tamm, L.K., *Hypothesis: spring-loaded boomerang mechanism of influenza hemagglutinin-mediated membrane fusion.* Biochem et Biophysica Acta, 2003. **1614**: p. 14-23.
- 15. Durell, S.R., et al., What studies of fusion peptides tell us about viral envelope glycoprotein-mediated membrane fusion (review). Mol Membr Biol, 1997. **14**(3): p. 97-112.
- 16. Peuvot, J., et al., Are the fusion processes involved in birth, life and death of the cell depending on tilted insertion of peptides into membranes? J Theor Biol, 1999. **198**(2): p. 173-81.
- 17. Gullion, T. and J. Schaefer, *Rotational-Echo Double-Resonance Nmr.* Journal of Magnetic Resonance, 1989. **81**(1): p. 196-200.
- 18. Dusold, S.S., A., *Dipolar Recoupling Under Magic-Angle Spinning Conditions*. Annual Reports of NMR Spectroscopy, 2000. **41**(185).
- 19. Long, H.W. and R. Tycko, *Biopolymer conformational distributions from solid-state NMR: alpha-helix and 3(10)-helix contents of a helical peptide.*Journal of the American Chemical Society, 1998. **120**(28): p. 7039-7048.

- 20. Han, X. and L.K. Tamm, *A host-guest system to study structure-function relationships of membrane fusion peptides.* Proceedings of the National Academy of Sciences of the United States of America, 2000. **97**(24): p. 13097-13102.
- 21. Bevington, P.R. and D.K. Robinson, *Data Reduction and Error Analysis for the Physical Sciences*. 1992, Boston: McGraw-Hill.
- 22. Zhang, H., Stephen Neal, and David S. Wishart, *RefDB: A database of uniformly referenced protein chemical shifts.* Journal of Biomolecular NMR, 2003. **25**: p. 173-195.
- 23. Han, X., L. K. Tamm, *pH-dependent Self-association of Influenza Hemagglutinin Fusion Peptides in Lipid Bilayers*. Journal of Molecular Biology, 2000. **304**: p. 953-65.
- 24. Vaccaro, L., K. J. Cross, J. Kleinjung, S. K. Straus, D. J. Thomas, S. A. Wharton, J. J. Skehel, and F. Fraternali, *Plasticity of Influenza Haemagglutinin Fusion Peptides and Their Interaction with Lipid Bilayers*. Biophysical Journal, 2005. **88**: p. 25 36.

Chapter Five
Summary and Future Work

5. Summary and Future Work

5.1 Summary

Membrane fusion is a very important natural process. In influenza, fusion is facilitated by the influenza viral hemagglutinin protein (HA)[1]. The amino terminus of the HA₂ domain of the hemagglutinin protein is known as the 'fusion peptide' because it has been shown to be important in viral/host cell membrane fusion and infection [2-6]. The free fusion peptide has been shown to cause membrane fusion in a pH-dependent way similar to the complete protein, making it a convenient model for the study of membrane fusion in influenza [7-10]. This research is focused on gaining understanding into how membrane fusion is induced/catalyzed by the influenza fusion peptide.

Because of the relatively low aqueous solubility of the fusion peptide, host-linked fusion peptides were synthesized [11, 12]. These peptides were much more soluble than the free fusion peptide, but were able to induce lipid mixing in liposomes in a pH-dependent way, similar to the free fusion peptide.

A partial crystal structure of the low-pH activated HA2 domain exists, but there is no atomic resolution structural data for the membrane bound form of the N-terminus fusion peptide [13]. Circular Dichroism, solution NMR, and EPR data sugggest that the fusion peptide inserts into micelles with a predominantly helical structure at the pH of fusion [11, 14-16].

Although the influenza fusion peptide has been studied extensively, variations in sample preparation and lipid composition are common. Therefore,

the effects of lipid composition, peptide:lipid ratio, temperature, and pH on the membrane bound fusion peptide structure were studied. REDOR subtraction was employed to filter out the large natural abundance ¹³C carbonyl signals from our spectra [17].

Our data show that there are at least two distinct structures of the membrane bound influenza fusion peptide. The structure is dependent on the lipid and cholesterol composition of the membranes with which it is associated. We have also found that the fusion peptide causes pH-dependent lipid mixing regardless of its equilibrium structure. This shows that there are at least two distinct structures of the influenza fusion peptide that can induce fusion.

Despite the extensive study of the fusion peptide, there is some variation between proposed fusion peptide structures. Some groups have observed helical structure at low pH for the peptide in DPC detergent solution by NMR, and for the peptide in POPC:POPG by ESR, IR, and CD [12, 15, 18-20]. While some groups report no change in helix orientation and no apparent structural change between high and low pH structures by EPR [18, 21], other groups have proposed considerable changes in the fusion peptide structure between low and high pH [15, 22]. We used REDOR to probe for a C-terminal 3₁₀ helix proposed by solution NMR to be present at low pH but absent at neutral pH [12]. Our REDOR experiments demonstrate that this structural feature is present in influenza fusion peptide at both low and neutral pH when the peptide is bound to DPC micelles or with POPC:POPG membranes. This conclusion is supported by

our chemical shift measurements, which suggest that there is no pH-dependent structure in the region.

There are at least two possible explanations for the promotion of membrane fusion in influenza. One is that the fusion peptide mechanically perturbs membranes to induce lipid mixing. The other is that the peptide acts as a space filler to stabilize perturbed membranes. Because we see no evidence for a significant pH-induced structural change in the fusion peptide, I support a model in which the fusion peptide acts as a space filler between hydrophobic lipid tails to stabilize the perturbed membranes and to catalyze fusion [23, 24]. The pH dependence of influenza fusion peptide might then be caused by changes in the peptide's structural rigidity, or by the protonation of acidic groups on the fusion peptide.

There is still a great deal of research to be done on membrane-associated influenza fusion peptides. Advances in NMR hardware and pulse sequences make it possible to work toward the structure of a uniformly labeled, membrane-associated, fusion peptide sample. The equilibrium structure of the entire influenza fusion peptide associated with lipid membranes and both neutral and low pH might give insight into the pH dependence of influenza fusion peptide fusion activity. In addition, work is being done in the Weliky group towards structural data on selectively labeled, membrane-associated samples using larger fragments of the fusion protein. This data could be used to look at the fusion peptide structures in the context of the larger protein. The effect of the

peptide (and protein) on lipid bilayer structure needs to be studied more extensively as well.

Understanding membrane fusion is an ambitious goal because the time scale of the fusion process is much shorter than the time scale required to make structural measurements. Therefore, I think that computer simulation and modeling will also be helpful in studying the specific interactions that underlie the molecular mechanisms of membrane fusion in influenza virus.

5.2 References

- 1. Hughson, F.M., *Structural Characterization of Viral Fusion Proteins*. Current Biology, 1995. **5**(3): p. 265-74.
- 2. Daniels, R.S., J. C. Downie, A. J. Hay, M. Knossow, J. J. Skehel, M. L. Wang, and D. C. Wiley, *Fusion Mutants of the Influenza Virus Hemagglutinin Glycoprotein*. Cell, 1985. **40**: p. 431 439.
- 3. Gething, M.J., R. W. Doms, D. York, and J. White, Studies on the Mechanism of Membrane Fusion: Site-Specific Mutagenesis of the Hemagglutinin of Influenza Virus. Journal of Cell Biology, 1986. 102: p. 11 23.
- 4. Olrich, M., and R. Rott, *Thermolysin Activation Mutants with Changes in the Fusogenic Region of an Influenza Virus Hemagglutinin*. Journal of Virology, 1994. **68**: p. 7537 7539.
- 5. Walker, J.A., and Y. Kawaoka, *Importance of Conserved Amino Acids at the Cleavage Site of teh Haemagglutinin of a Virulant Avian Influenza A Virus*. Journal of General Virology, 1993. **74**: p. 311 314.
- 6. Durrer, P., et al., *H+-induced membrane insertion of influenza virus hemagglutinin involves the HA2 amino-terminal fusion peptide but not the coiled coil region.* J Biol Chem, 1996. **271**(23): p. 13417-21.
- 7. Murata, M., Y. Sugahara, S. Takahashi, S-i. Ohnishi, pH-Dependent Membrane Fusion Activity of a Synthetic Twenty Amino Acid Peptide with the Same Sequence as That of the Hydrophobic Segment of Influenza Virus Hemagglutinin. Journal of Biochemistry, 1987. 102: p. 957-62.
- 8. Qiao, H., R. Todd Armstrong, Grigory B. Melikyan, Fredric S. Cohen, and Judith M. White, *A Specific Point Mutant at Position 1 of the Influenza Hemagglutinin Fusion Peptide Displays a Hemifusion Phenotype.*Molecular Biology of the Cell, 1999. **10**: p. 2759 2769.
- 9. Wharton, S.A., S. R. Martin, R. W. Ruigrok, J. J. Skehel, and D. C. Wiley, Membrane Fusion by Peptide Analogues of Influenza Virus Haemagglutinin. Journal of General Virology, 1988. **69**: p. 1847 - 1857.

- 10. Lear, J.D.a.W.F.D., *Membrane Binding and Conformational Properties of Peptides Representing the NH₂ Terminus of Influenza HA-2*. The Journal of Biological Chemistry, 1987. **262**(14): p. 6500-05.
- 11. Han, X., L. K. Tamm, *A host-guest system to study structure-function relationships of membrane fusion peptides.* Proceedings of the National Acadamy of Science, 2000. **97**(24): p. 13097-102.
- 12. Han, X., L. K. Tamm, *pH-dependent Self-association of Influenza Hemagglutinin Fusion Peptides in Lipid Bilayers.* Journal of Molecular Biology, 2000. **304**: p. 953-65.
- 13. Chen, J., J. Skehel, and D. C. Wiley, *N- and C-terminal residues combine in the fusion-pH influenza hemagglutinin HA₂ subunit to form an <i>N cap that terminates the triple-stranded coiled coil.* Porceedings of the National Acadamy of Science of the United States of America, 1999. **96**: p. 8967-72.
- 14. Chang, D.-K., S-F. Cheng, V. D. Trivedi, and S-H. Yang, *The Aminoterminal Region of the Fusion Peptide of Influenza Virus hemagglutinin HA2 Inserts into Sodium Dodecyl Sulfate Micelle with Residues 16-18 at the Aqueous Boundary at Acidic pH.* The Journal of Biological Chemistry, 2000. **275**(25): p. 19150-58.
- 15. Han, X., Bushweller, J. H., Cafiso, D. S., Tamm, L. K., *Membrane* structure and fusion-triggering conformational change of the fusion domain from influenza hemagglutinin. Nat Struct Biol, 2001. **8**(8): p. 715-20.
- 16. Tamm, L.K., Frits Abildgaard, Ashish Arora, Heike Blad, John H. Bushweller, Structure, Dynamics and Function of the outer Membrane Protein A (OmpA) and influenza Hemagglutinin Fusion Domain in Detergent Micelles by Solution NMR. FEBS Lett, 2003. 555: p. 139 143.
- 17. Yang, J., Parkanzky, P. D., Bodner, M. L., Duskin, C. G., Weliky, D. P., Application of REDOR Subtraction for Filtered MAS Observation of Labeled Backbone Carbons of Membrane-Bound Fusion Peptides.

 Journal of Magnetic Resonance, 2002. **159**(2): p. 101-110.
- 18. Macosko, J.C., C.H. Kim, and Y.K. Shin, *The membrane topology of the fusion peptide region of influenza hemagglutinin determined by spin-labeling EPR.* J Mol Biol, 1997. **267**(5): p. 1139-48.

- 19. Hsu, C.H., et al., Structural characterizations of fusion peptide analogs of influenza virus hemagglutinin Implication of the necessity of a helix-hinge-helix motif in fusion activity. Journal of Biological Chemistry, 2002. 277(25): p. 22725-22733.
- 20. Dubovskii, P.V., et al., *Structure of an analog of fusion peptide from hemagglutinin*. Protein Science, 2000. **9**(4): p. 786-798.
- Zhou, Z., J. C. Macosko, D. W. Hughes, B. G. Sayer, J. Hawes, and R. M. Epand, ¹⁵N NMR Study of the Ionization Properties of the Influenza Virus Fusion Peptide in Zwitterionic Phospholipid Dispersions. Biophysical Journal, 2000. **78**: p. 2418-25.
- 22. Tamm, L.K., *Hypothesis: spring-loaded boomerang mechanism of influenza hemagglutinin-mediated membrane fusion*. Biochem et Biophysica Acta, 2003. **1614**: p. 14-23.
- 23. Bentz, J., *Membrane Fusion Mediated by Coiled Coils: A Hypothesis.* Biophysical Journal, 2000. **78**: p. 886-900.
- Vaccaro, L., K. J. Cross, J. Kleinjung, S. K. Straus, D. J. Thomas, S. A. Wharton, J. J. Skehel, and F. Fraternali, *Plasticity of Influenza Haemagglutinin Fusion Peptides and Their Interaction with Lipid Bilayers*. Biophysical Journal, 2005. **88**: p. 25 36.

